



ELSEVIER

Contents lists available at ScienceDirect

Deep-Sea Research I

journal homepage: www.elsevier.com/locate/dsrI

Variability of SeaWiFS chlorophyll-*a* in the southwest Atlantic sector of the Southern Ocean: Strong topographic effects and weak seasonality

Jisoo Park^{a,b}, Im-Sang Oh^b, Hyun-Cheol Kim^c, Sinjae Yoo^{a,*}

^a Korea Ocean Research and Development Institute, 425-170 Sa-dong, 1270 Ansan, Republic of Korea

^b Seoul National University, Republic of Korea

^c Korea Polar Research Institute, Republic of Korea

ARTICLE INFO

Article history:

Received 7 July 2009

Received in revised form

11 January 2010

Accepted 25 January 2010

Available online 1 February 2010

Keywords:

Interannual variation

Seasonality

SeaWiFS chlorophyll-*a*

Southern Ocean

Topographic effect

ABSTRACT

This study examined 11-year (1997–2008) weekly and monthly time series of satellite-observed ocean color to understand the dominant temporal and spatial patterns of chlorophyll-*a* in the southwest Atlantic sector of the Southern Ocean. Using empirical orthogonal function analysis and *k*-means classification, we classified the study area into eight regions, which were in good accordance with the oceanographic and topographic features. Examination of the chlorophyll-*a* time series in each region revealed that contrary to our expectation, regular seasonal phytoplankton blooms were observed only in a limited area. Of the eight regions, only two showed typical seasonal blooms, and one showed weak seasonality, whereas other regions exhibited irregular seasonal blooms of variable duration. We attribute the absence of regularity in seasonal blooms to relatively shallow winter mixing, which would prevent entrainment of limiting micronutrients such as iron and silicate. In the southwest Atlantic sector of the Southern Ocean, topographic effects and sea ice may be the most important factors controlling primary productivity. In the South Georgia region, chlorophyll-*a* showed a significant correlation with geostrophic current velocity, indicating that topographic effects depend on the interaction of current strength and topographic structure. Interannual variability of the surface chlorophyll in some regions also revealed longer periodicity (~6 years). The periodicity seemed to be related to El Niño–Southern Oscillation and to sea-ice dynamics influenced by the Antarctic Circumpolar Current.

© 2010 Elsevier Ltd. All rights reserved.

1. Introduction

Although the Southern Ocean (SO) represents only 10–20% of the area of the world ocean, it may play a unique and important role in controlling global climate by altering the carbon cycle (Sarmiento et al., 1998; DiTullio et al., 2000; Bopp et al., 2001; Honjo, 2004; Gille, 2002; El-Sayed, 2005). The SO (south of 50°S) accounts for about 20% (0.47 GtCyr⁻¹) of the global CO₂ sink (Takahashi et al., 2002), and the export flux of particulate organic carbon is significant compared with that of the global ocean (Schlitzer, 2002). The SO regulates global nutrient distribution in most of the upper ocean (Sarmiento et al., 2004). Phytoplankton blooms, in particular, play a key role in export of carbon to the bottom layer and drawdown of atmospheric CO₂, and the SO has been acknowledged as the most important region for the export and burial of biogenic silica (Treguer et al., 1995). However, Antarctic waters are also characterized by low phytoplankton

abundance and low rates of primary production in spite of high concentrations of inorganic macronutrients (Mitchell and Holm-Hansen, 1991; Chisholm and Morel, 1991). This condition has been referred to as the high-nutrient low-chlorophyll (HNLC) paradox (Chisholm and Morel, 1991). Typical chlorophyll-*a* concentrations in the SO range between 0.05 and 1.5 mg m⁻³ (Arrigo et al., 1998; El-Sayed, 2005; Marrari et al., 2006), and according to Marrari et al. (2006), 96% of the satellite-estimated chlorophyll-*a* in the surface waters falls within this range. On the other hand, in the southwest Atlantic sector of the SO (SASSO), a full gamut of productivity exists, ranging from typical HNLC areas to very productive areas in the South Georgia region (Atkinson et al., 2001).

Another aspect of the primary production of the SASSO is its role in supporting ecosystem functions. The South Georgia region is well known for its wealth of life, including krill, fish, and vertebrate predators. Krill is an important consumer of the primary production linking lower and higher trophic levels (Murphy et al., 2007). The potential krill biomass in the SO was found to range from 67 to 297 million tons (Siegel, 2005), and krill stock biomass varied interannually by one order of magnitude

* Corresponding author. Tel.: +82 31 4006221; fax: +82 31 4085934.
E-mail address: sjyoo@kordi.re.kr (S. Yoo).

between consecutive years (Brierley et al., 1999; Atkinson et al., 2001). Furthermore, more than half of the SO krill stocks are concentrated in the SASSO, and summer krill density was shown to be significantly correlated with chlorophyll-*a* concentration in that region (Atkinson et al., 2004, 2008; see also Siegel, 2005). Are krill dynamics responding to the seasonal cycles and the interannual variations of primary production as in other parts of the world ocean?

Geographic and topographic features of the SASSO include the Drake Passage and the Scotia Arc (Fig. 1). The Scotia Arc consists of the North Scotia Ridge, South Georgia Island, South Sandwich Islands, South Scotia Ridge, and South Orkney Island. The Drake Passage acts as a bottleneck for the Antarctic Circumpolar Current (ACC), and the Scotia Arc acts as a barrier to the ACC. Together, these features form a sack-like shape and create a very complicated circulation pattern and oceanographic conditions, which in turn affect biological processes, including organic production.

Phytoplankton biomass and productivity in the SASSO are characterized by low pigment biomass and production rates around the Drake Passage, in contrast with high chlorophyll-*a* and production rates in regions influenced by the Shackleton Transverse Ridge, as well as in the coastal area, frontal mixing zone, seasonal ice zone, and area downstream of South Georgia (reviewed by Atkinson et al., 2001; Holm-Hansen et al., 2004). For example, high chlorophyll-*a* concentrations (up to 25 mg m^{-3}) were observed within Marguerite Bay (Meyer et al., 2003) and in the marginal ice zone (up to 7 mg m^{-3} ; Arrigo and van Dijken, 2003) and around South Georgia ($> 10 \text{ mg m}^{-3}$; Atkinson et al., 2001; Korb et al., 2004).

Estimates of primary production of the SASSO region based on recent data (1990s) revealed large variability both temporally and spatially, with values ranging from 111 to $6000 \text{ mgC m}^{-2} \text{ d}^{-1}$ (Mitchell and Holm-Hansen, 1991; Savidge et al., 1995; Bracher et al., 1999; Dierssen et al., 2000; Moore and Abbott, 2000; Strass et al., 2002; Holm-Hansen et al., 2004; Smith et al., 2008). Phytoplankton blooms in the South Georgia region can be sustained for 4–5 months (Atkinson et al., 2001; Ward et al., 2002), whereas blooms are brief in October/November in the Southern Antarctic Circumpolar Current Front (SACCF) region of the western Antarctic Peninsula (AP; Smith et al., 2008).

Thus, the diversity of the SASSO provides us with a means to study the mechanisms of chlorophyll-*a* dynamics over a wide range of environmental settings and physical forcings. The major

objectives of this study were as follows: (1) to classify biological domains using satellite-observed chlorophyll-*a* over an extended region that includes the Antarctic Peninsula, Drake Passage, Scotia Sea, and area downstream of South Georgia; (2) to analyze the spatial patterns and seasonal-to-interannual variability of chlorophyll-*a* in the study area; and (3) to identify possible mechanisms that could control the seasonal pattern of phytoplankton dynamics in each region.

2. Data and materials

2.1. Study area and data screening

Fig. 1 shows the study area (SASSO) with its bathymetry. Because of the low solar elevation and sea-ice coverage in winter, data are missing in some areas. We confined our analysis to the area in which more than 50% of valid chlorophyll-*a* pixels were available for the study period, which excluded the Weddell Sea. We also intentionally excluded the Patagonia Basin and the region west of South America from this analysis.

2.2. Chlorophyll-*a*

Sea-viewing Wide Field-of-view Sensor (SeaWiFS)-derived estimates of surface chlorophyll-*a* concentrations for the period from September 1997 through December 2007 were obtained from the Goddard Space Flight Center (McClain et al., 1998). Moderate-Resolution Imaging Spectroradiometer (MODIS) Aqua data were also obtained for the period from January 2008 to August 2008 to supplement missing data. In this study, we used Level 3 (L3) 8-d data as well as monthly averaged global data sets. Because ocean color data are not available in the SO in winter because of the low solar elevation, we used only 6 months of data per year (October–March) for analysis. The spatial resolution of SeaWiFS and MODIS chlorophyll-*a* data is 12 by 12 pixels in a degree (about 9 km latitudinally and 5.5 km longitudinally per pixel in the central region of the study area).

2.3. Sea ice

Monthly mean sea-ice concentrations were from NASA's Scanning Multichannel Microwave Radiometer (SMMR) and the

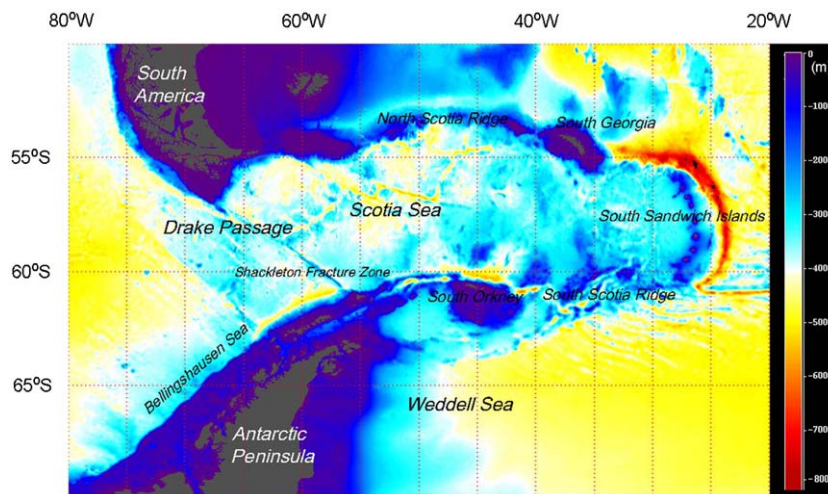


Fig. 1. A bathymetry map of the southwest Atlantic sector of the Southern Ocean. The North Scotia Ridge, South Georgia Island, South Sandwich Islands, South Scotia Ridge, and South Orkney Island make up the Scotia Arc. The map was drawn using SeADAS program.

Spectral Sensor Microwave/Imager (SSM/I) of the Defense Meteorological Satellite Program (DMSP), where sea-ice concentrations were determined using the NASA Team algorithm. Data from the DMSP's F13 satellite for the same periods as chlorophyll data were obtained from the Earth Observing System Data and Information System (EOSDIS), National Snow and Ice Data Center (NSIDC) Distributed Active Archive Center, University of Colorado, Boulder. Ice concentrations < 15% were considered to be open water in our analysis (Gloersen et al., 1992; Smith et al., 1998; Stammerjohn et al., 2008). We used only data that overlapped temporally with the satellite-derived chlorophyll-*a*.

2.4. Mixed layer depth

As the climatological mixed layer depth (MLD), we used data for the world ocean (de Boyer Montegut et al., 2004), calculated based on direct MLD estimates from individual profiles. These data can be downloaded from the website <http://www.locea.n-ipsl.upmc.fr/~cdblod/mld.html>. Here, the MLD was defined as the depth at which temperature changes by 0.2 °C relative to that at a near-surface reference depth.

2.5. Geostrophic current

The Ssalto/Data Unification and Altimeter Combination System (Duacs) multimission altimeter products used for the geostrophic current were distributed by the Archiving, Validation and Interpretation of Satellite Oceanographic data (AVISO) service, with support from the Centre National d'Études Spatiales (CNES, <http://www.aviso.oceanobs.com/duacs/>). The Ssalto/Duacs system processes data from all altimeter missions (Jason 1 and 2, Topex/Poseidon [T/P], Envisat, GEOSAT Follow-on [GFO], European Remote Sensing [ERS] satellites 1 and 2, and Geosat). We used the gridded "absolute geostrophic velocity" data, which are provided at 7-d intervals on a $(1/3)^\circ \times (1/3)^\circ$ Mercator grid (with the same resolution in latitude and longitude). The weekly data were composited to monthly data for comparison with chlorophyll-*a* data.

2.6. Other remote sensing data

For the sea surface temperature (SST), National Oceanic and Atmospheric Administration Advanced Very High Resolution Radiometer (NOAA AVHRR) data were acquired from the Physical Oceanography Distributed Active Archive Center (PO.DAAC) at the Jet Propulsion Laboratory/Caltech, and MODIS data were also obtained for the recent period. The temporal resolution of these data was about 9 km per pixel. For sea surface wind data, Quick Scatterometer (QuikSCAT) wind measurements (version 3.0) were downloaded from Remote Sensing Systems in Santa Rosa, California (<ftp.ssmi.com>). The spatial resolution of the data was 0.25° per pixel, with 1440 × 720 arrays for global coverage; monthly composite data were used here. The data consisted of wind speed, wind direction, and a rain flag. The rain-contaminated pixels were eliminated before use. In addition, SeaWiFS-derived estimates of surface photosynthetically available radiation (PAR) for the same period as the chlorophyll-*a* data were also used. The attenuation coefficient of PAR (KPAR) was derived from the SeaWiFS k490 data using in situ PAR profiles (2001–2005; unpublished data).

2.7. Climate indices

The Southern Oscillation Index (SOI) is calculated from the monthly or seasonal fluctuation in the air pressure difference

between Tahiti and Darwin, Australia. This index is anti-correlated with the Multivariate El Niño–Southern Oscillation (ENSO) Index (MEI) and is not significantly different. Positive values of the SOI are associated with stronger Pacific trade winds and warmer sea temperatures to the north of Australia, popularly known as a La Niña episode. We downloaded the SOI data from the following website: <http://www.bom.gov.au/climate/glossary/soi.shtml>. The Southern Hemisphere Annular Mode (SAM) is an expression of the meridional pressure gradient between the sub-Antarctic and middle latitudes. We used an observation-based SAM index (Marshall, 2003), for which data can be obtained from the website <http://www.antarctica.ac.uk/met/gjma/sam.html>.

2.8. Empirical orthogonal function analysis and classification into subregions

Empirical orthogonal function (EOF) analysis was applied to chlorophyll-*a* data without subtracting means to retain information on seasonality. We used the *k*-means algorithm to classify the SASSO into subregions using the EOFs of chlorophyll-*a* variations. The *k*-means algorithm is designed to place observed data points into "*k* clusters" in which each observed data point belongs to the cluster with the nearest mean. See MacKay (2003) for more details.

3. Results

3.1. Chlorophyll-*a* climatology

Fig. 2 presents monthly chlorophyll-*a* climatology maps during austral summer with mean sea-ice extent for each month. Generally, chlorophyll-*a* begins to increase from September, and blooms continue from October through February. Large regional variation is shown in the timing of peaks. In summer, phytoplankton blooms with chlorophyll-*a* values exceeding 1.0 mg m^{-3} are shown in several regions, with the highest values associated with bottom topography, i.e., islands, submerged plateaus, and ridges, as will be discussed in Section 3.5. In addition, chlorophyll-*a* values are high in the marginal ice zone. Throughout much of the SO, the sea-ice edge and the zones and fronts of the ACC lie roughly parallel, following the lines of latitude (Atkinson et al., 2001). Sea-ice retreat starts in October and November and is faster to the west of the AP. Sea-ice extent reaches its minimum in February and advances from the Weddell Sea region in March. By March, blooms begin to disappear.

3.2. Classification of the biological domain

We computed EOFs from the 11-year monthly time series (total 66 months) of SeaWiFS/MODIS chlorophyll-*a* data to examine the dominant spatial and temporal patterns. Fig. 3 shows the three largest EOF modes. The first mode described phytoplankton blooms in December in the northern region of the Drake Passage and explained 19.1% of the variability. The time series of EOF amplitudes in each year are mostly regular, indicating a strong seasonality in the region. In other words, the timing of seasonal chlorophyll-*a* peaks was regular. The second mode described early phytoplankton blooms in November triggered by ice retreat in the southern region of the Drake Passage and in the Scotia Sea along the SACCF and the southern boundary of the ACC (SB), explaining 11.1% of the variability. The time series of the second-mode amplitudes were more variable than were those of the first mode. The third mode described late blooms in the northern Scotia Sea (nSC) region and explained 8.6% of the variability. Again, the seasonal pattern was more variable

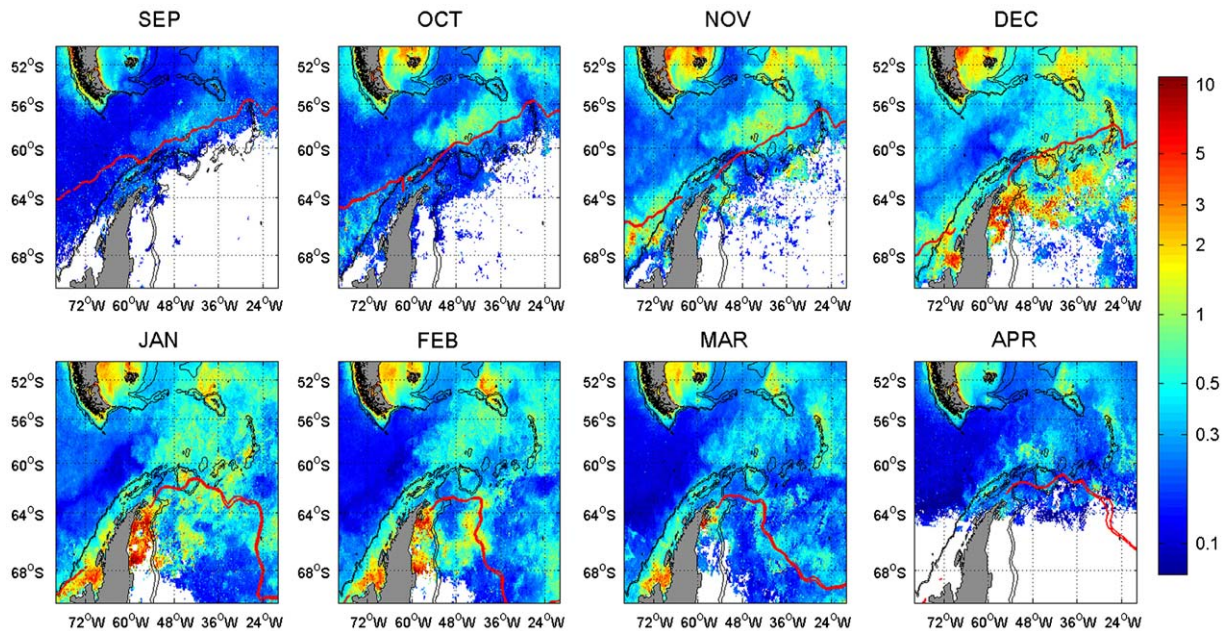


Fig. 2. Monthly chlorophyll-*a* climatology of the southwest Atlantic sector of the Southern Ocean (11-year mean). Color shows SeaWiFS and MODIS chlorophyll-*a* concentration calculated by a standard algorithm. Black lines represent 1000- and 2000-m isobaths. Red lines represent 11-year-mean sea-ice extent in each month. White areas indicate data limited by sea-ice coverage or low solar elevation (see also Fig. 3).

than that of the first EOF mode. This pattern was most prevalent along the AP and nSC (see also Fig. 5a). The first three modes represent regular seasonal patterns and as a whole account for 38.8% of the variance. The remaining modes do not show seasonally regular patterns (data not shown). Thus, a large portion of the chlorophyll variability in the region cannot be attributed to regularly occurring seasonal peaks.

We then classified the regions based on the temporal characteristics of the EOFs. The first eight EOFs with associated variance greater than 3% were chosen. In total, these eight EOFs explained approximately 60% of the variance. The *k*-means algorithm was applied to seven, eight, and nine EOFs, which resulted in more or less similar patterns. After trial and error, we found that eight patterns best described and represented the known oceanographic characteristics of the study region (Fig. 4). In Fig. 4, different colors of shading depict the eight regions with the major fronts overlaid. As shown in the figure, fronts such as the Polar Front (PF), SACCF, and SB separate the regions. The PF separates the southern and northern Drake Passage regions (sDP and nDP in Fig. 5a). The shelf region of the AP is also well delimited by the SACCF and the SB. Other topographic features further demarcate the regions. For example, the western Scotia Sea (wSC) is delimited by the Shackleton Fracture Zone (SFZ) and Pirie Bank (PB) as well as the PF and the SB. The North Scotia Ridge, South Sandwich Islands, and South Georgia Island also form boundaries separating different regions. The nSC and eastern Scotia Sea (eSC) regions, as defined in Fig. 5a, are separated by bottom topography.

These eight patterns can be characterized by chlorophyll-*a* dynamics, whose peak timing closely matches the eight patterns (Fig. 5a). The seasonal maximum (Fig. 5b) and minimum chlorophyll-*a* (not shown) also show good correspondence with the eight patterns. For example, the sDP area is characterized by an earlier peak (November) and low chlorophyll-*a* ($< 0.4 \text{ mg m}^{-3}$). While peak concentrations were low, they were still greater than the minimum concentrations by more than two-fold. On the other hand, the South Georgia (SG) region has the highest chlorophyll-*a* ($> 3.0 \text{ mg m}^{-3}$) and late peaks (December–February).

Chlorophyll-*a* also peaked in November in the eSC. Chlorophyll-*a* peaked in the middle of summer in the nDP and nSC (in January). Late timing of maximum chlorophyll-*a* was found in the South Sandwich Islands (SSW) region and the eastern part of the AP region (in February).

The eight patterns also show characteristic seasonal maximum chlorophyll-*a* concentrations. The high chlorophyll-*a* concentration ($> 3 \text{ mg m}^{-3}$ in the Georgia Basin) contrasts with the low concentration in the Drake Passage and nSC regions ($\sim 0.3 \text{ mg m}^{-3}$ in the Drake Passage and nSC), with an order of magnitude difference. Chlorophyll-*a* concentrations in the central region of the SC and east of the South Sandwich Islands were also relatively high ($1\text{--}1.5 \text{ mg m}^{-3}$). Low surface temperature, weak density stratification, weak light intensity, low iron concentration, strong wind stress, and grazing pressures all contribute to the low biomass of phytoplankton in the ACC region (Bathmann et al., 1997; Bracher et al., 1999; Holm-Hansen et al., 2004; see also Mitchell and Holm-Hansen, 1991), whereas enhanced supply of iron and rapid recycling of nitrate could contribute to the high phytoplankton biomass in the SG region (Atkinson et al., 2001; Wulff and Wangberg, 2004). The spatial distribution of seasonal minimum concentrations of chlorophyll-*a* was not significantly different from that of peak-time concentrations, with an order of magnitude difference in the high-productivity regions (data not shown).

3.3. Seasonal cycles in the eight regions

To understand the temporal changes of surface chlorophyll-*a*, we defined regions (Fig. 5a) based on the eight patterns (Fig. 4). From each region, we extracted time series of median values of chlorophyll-*a* concentration using 8-d composite data (Fig. 6). Seasonal variability of chlorophyll-*a* was high in the eight regions. Of the eight regions, regular seasonal cycles are evident only in the sDP and nDP. With the exception of a few years, peaks occurred in November (sDP) or in December (nDP). In the nSC, peaks usually occurred between December and February. In other

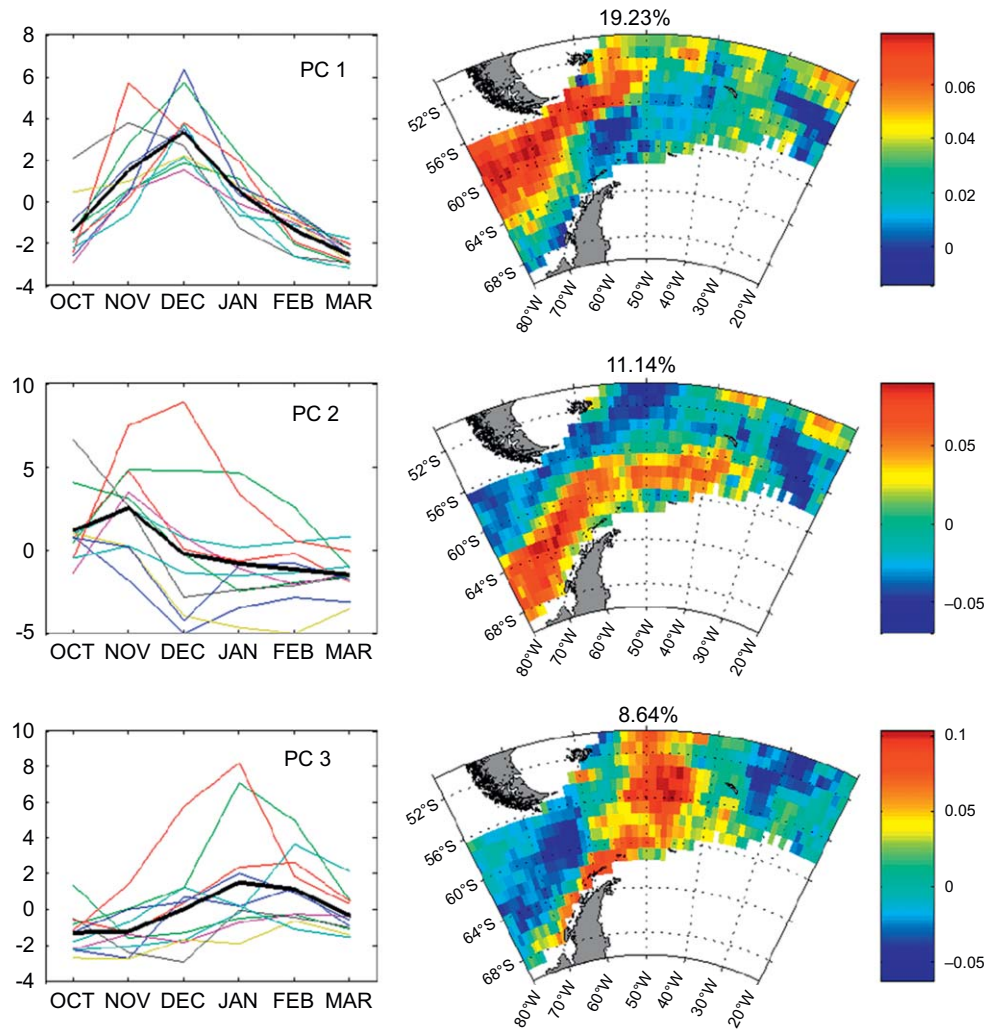


Fig. 3. Principle components (PCs: left panels) and spatial patterns (EOFs: right panels) of the monthly chlorophyll-*a* concentration showing the three largest modes. Colors represent 11 PCs for each year, and thick black lines show the average value of PCs (left panels). Percents indicate the amount of total variance described by each mode (right panels).

regions, the timing of the peaks was irregular, or multiple peaks occurred in a year.

The earliest spring blooms began in the sDP, wSC, eSC, and SG regions (Figs. 6a, f, g, h). These regions are bounded by the PF and SB. Subsequent chlorophyll peaks reappeared in late summer in these regions, except in the sDP. Blooms continued longer than 2–3 months from December to March with irregular timing every year. According to the Ward et al. (2002) study, the duration of the phytoplankton bloom was about 82–122 d in the ACC and around South Georgia Island.

Seasonality can also be examined from Fig. 7, in which time series of 8-d chlorophyll-*a* composites are shown for the October–March period from 1997 to 2008. In the sDP and nDP, spring blooms occurred regularly. In the nSC, in some years (1998/1999, 1999/2000, 2001/2002, 2003/2004, 2006/2007), blooms occurred regularly in January but not in other years. In other regions, regular seasonality is not evident.

Table 1 summarizes the characteristics of chlorophyll variability and oceanographic features in the eight regions. In the table, the range of peak chlorophyll-*a* concentrations is shown. The regions are arranged in the order of increasing maximum chlorophyll levels. Seasonality is determined by the regularity of timing of chlorophyll-*a* peaks. For example, in the sDP and nDP, a single seasonal peak occurs at a similar time of

the year showing a strong seasonality (see also Fig. 6). On the other hand, in SSW, wSC, eSC, and SG, multiple peaks occur at different times of the year (no seasonality). Except for the AP, where an unusually high chlorophyll-*a* event occurred in 2005/2006, as the chlorophyll-*a* level increases, the seasonality weakens and disappears.

3.4. Interannual variations

Some peculiar peaks occurred in different years (Fig. 6). The 2005/2006 peaks in the sDP (Fig. 6a), AP (Fig. 6b), SSW (Fig. 6e), and wSC (Fig. 6f) seemed to be related to the blooms associated with ice retreat (see Discussion). The peaks in 1997/1998 and 2004/2005 in the nDP (Fig. 6c) appeared to be related to eddy activities. The peaks in the SG region in 1999/2000, 2002/2003, and 2003/2004 (Fig. 6h) were related to a stronger ACC. Possible causes of these particular peaks are explained in Section 3.5. Fig. 7 also shows different patterns of interannual variability of chlorophyll-*a* in each region. Generally, in most regions except the SSW and SG, the chlorophyll-*a* level was low in 2001/2002 and 2002/2003 (Figs. 6e, h). On the other hand, chlorophyll-*a* was high in the sDP and nDP during the two El Niño years (1997/1998 and 2004/2005; Figs. 6a, c). In the AP, an intense bloom with a

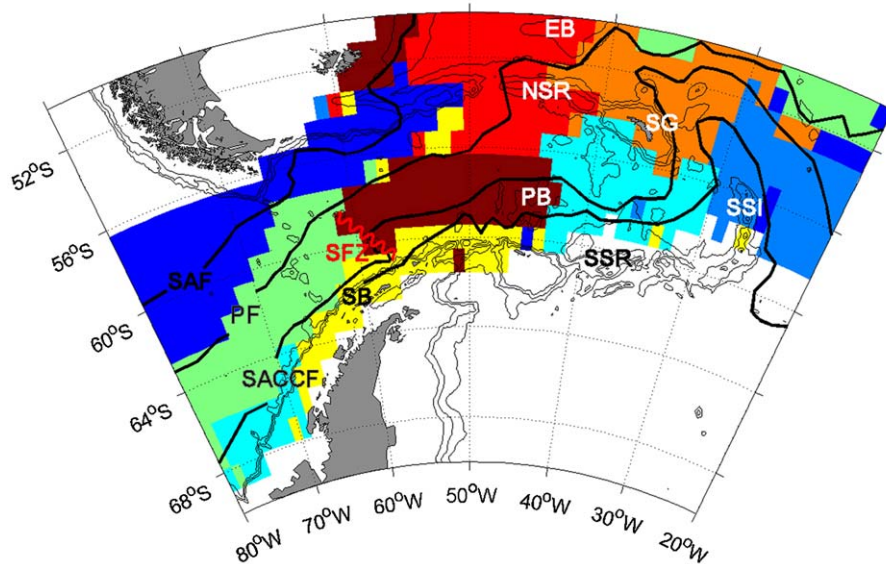


Fig. 4. Classification of the eight regions by the *k*-means algorithm based on the eight largest PCs (which capture about 60% of the variance) of monthly chlorophyll-*a* concentration. Black lines indicate 1000-, 2000-, and 3000-m isobaths. The four thick lines represent the approximate locations of the sub-Antarctic Front (SAF), Polar Front (PF), Southern Antarctic Circumpolar Current Front (SACCF), and southern boundary of the ACC (SB) (after Orsi et al., 1995; Moore et al., 1997; see also Meredith et al., 2003). Topographic barriers are also depicted (PB—Pirie Bank; SFZ—Shackleton Fracture Zone; EB—Ewing Bank; NSR—North Scotia Ridge; SSR—South Scotia Ridge; SG—South Georgia Island; SSI—South Sandwich Islands).

median chlorophyll-*a* value of 1.989 mg m^{-3} (by comparison, the second largest value was 0.588 mg m^{-3} in other years) appeared in January 2006 (Fig. 6b), which will be addressed again in the Discussion section. Seasonal to interannual variations of chlorophyll-*a* in the Scotia Sea and South Georgia regions had very different patterns from those in other regions.

To compare the interannual variations of overall chlorophyll-*a* levels in each region, seasonally averaged (October–March) chlorophyll-*a* concentrations and peak timing are shown in Fig. 8. Except in the nDP and nSC, interannual differences in the seasonal mean of chlorophyll-*a* were large. In the SG region, for example, the maximum (1.177 mg m^{-3} in 2001/2002) was more than three times higher than the minimum (0.373 mg m^{-3} in 2006/2007). Considering primary production is largely proportional to chlorophyll-*a* concentrations, the differences can be significant in terms of ecosystem function. We can also recognize peaks in 2005/2006 in the sDP, AP, and wSC, representing large blooms related to ice retreat (see Discussion). In the wSC, and to a lesser degree in the sDP and AP, two cycles (high during 1998–2001 and in 2005/2006, but low in 1997/1998 and 2002/2003) can be recognized, although the total period is not long enough to draw firm conclusions. We will discuss a possible link of this periodicity to ENSO in the Discussion section. The strong seasonality in the nDP and sDP can also be recognized in the peak timing. In the wSC, eSC, and SSW, peak timing was quite variable, ranging from October to March. However, it should be noted that multiple peaks occurred in all the regions except for the sDP and nDP; here, the peak timing indicates the timing of the largest peak of the year.

3.5. Topographic effects

Island effects refer to the enhancement of productivity by hydrodynamic changes (fronts, eddies, shoaling of the MLD) induced by island masses that bring nutrients to the upper mixed layer (UML) or by inorganic nutrients supplied from islands themselves (Blain et al., 2007). Similar effects can be produced by

submerged plateaus and ridges. We refer to topographic effects in a broader sense that includes island effects and similar effects from other submerged topographic features. The fact that the eight regions have distinctive temporal patterns of chlorophyll-*a* and are bounded by topographic features indicates that topographic effects are very important in the SASSO. In fact, the maximum chlorophyll-*a* distribution shows good correspondence with circulation patterns and topographic features (Fig. 5b). Three features are pronounced in Fig. 5b. First, the overall pattern coincides with the krill biomass distribution (Atkinson et al., 2004). Second, the higher chlorophyll-*a* concentrations correspond with topographic features: along the shelf area of the AP; over the SFZ (A in Fig. 5b) and PB (B); in the wake of South Georgia Island (C); and around the South Sandwich (D) and South Orkney (E) Islands. Third, the higher chlorophyll-*a* concentrations occur mostly to the south of the PF and to the north of the SB except for the Antarctic Peninsula shelf, which is under the influence of the shallow topography and sea ice. Topographic effects are not evident to the north of the PF in the northern Scotia Ridge area and in the South Scotia Ridge region, which is mostly south of the SB. Thus, large-scale topographic effects seem to result from the interaction of topographic features (A–C) and the ACC. The enhanced chlorophyll-*a* concentrations in the SSW region (D) and the South Orkney Islands (E) are due to local island effects not associated with the ACC.

The general circulation of the SASSO is dominated by the eastward flow of the ACC under the prevailing easterly winds throughout the year. In the Drake Passage, the ACC passes over the SFZ, a topographic barrier, which induces vertical mixing. For example, in the east of the SFZ, a phytoplankton bloom occurred in early spring, and this bloom spread out to the east in 1998 (Fig. 9a). The maximum chlorophyll-*a* map (Fig. 5b) suggests the influence of the SFZ. In the nDP, eddies were also observed, enhancing the chlorophyll-*a* level in 1998/1999 and 2004/2005 (see also Fig. 6c). In Fig. 9b, anticyclonic eddies are shown with low chlorophyll-*a* in the core but increased chlorophyll-*a* in the surroundings in December 2004. Here the existence of cyclonic and anticyclonic eddies was double-checked with maps of sea-level anomaly.

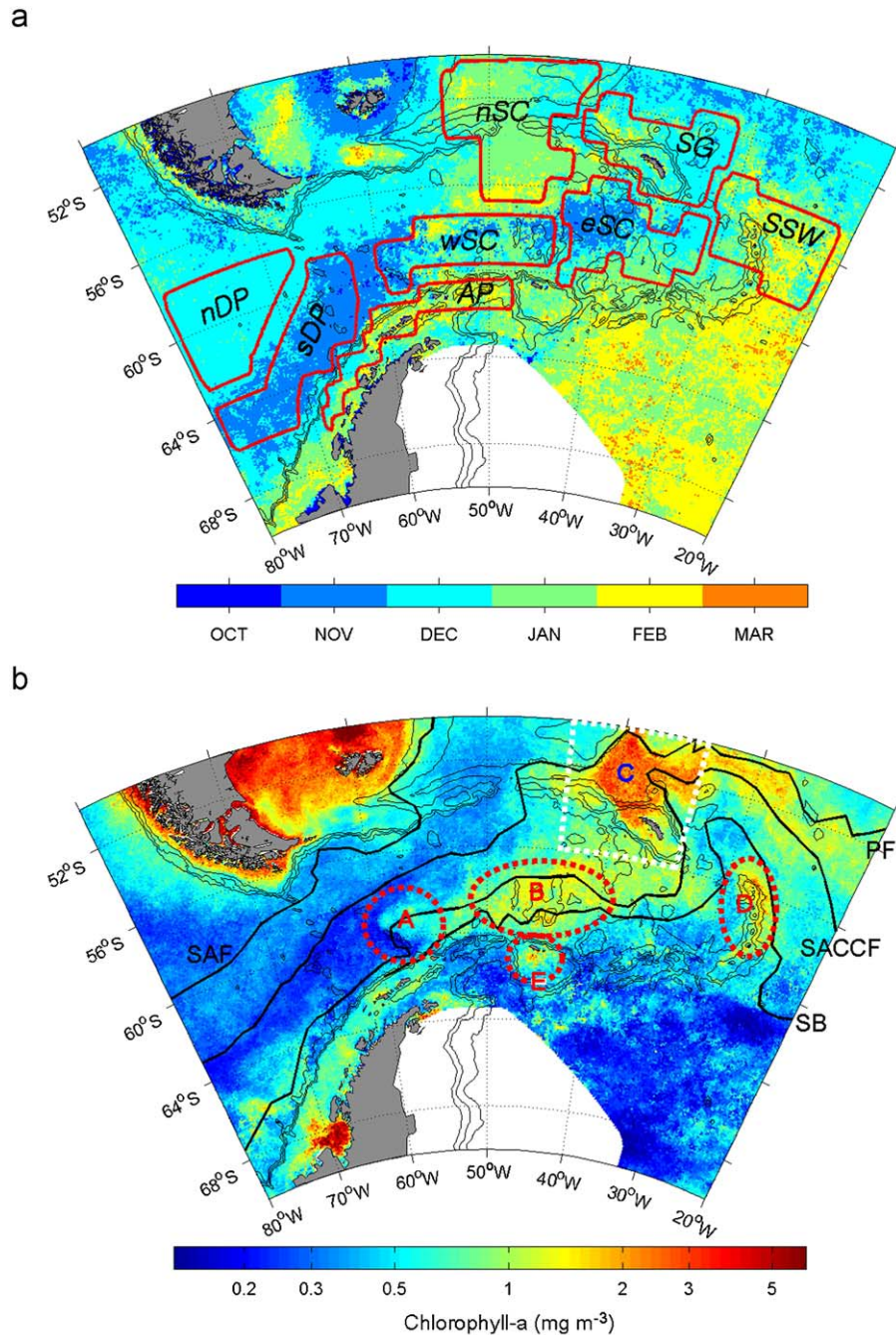


Fig. 5. Eight regions of interest for extracting time-series data (denoted by red polygons): nDP: northern Drake Passage region; sDP: southern Drake Passage region; AP: northern Antarctic Peninsula region; wSC: western Scotia Sea region; nSC: northern Scotia Sea region; eSC: eastern Scotia Sea region; SG: South Georgia region; and SSW: South Sandwich Islands region. (a) Timing of the annual maximum in chlorophyll-*a*. (b) Seasonal maximum chlorophyll-*a* concentrations (mg m^{-3}). A–E indicate the regions where topographic effects are pronounced. See the text for further explanation. The rectangle outlined by white dotted lines is the area where chlorophyll and geostrophic currents were extracted for Figs. 10 and 11. The timing and maximum concentrations were calculated from the median value of the 11 annual chlorophyll-*a* maximum values at each pixel from October 1997 to March 2008. Three major fronts and isobaths are also depicted.

To the east of Drake Passage, the ACC encounters one of the biggest topographic barriers in the SO. The Scotia Sea has a deep basin that is semi-enclosed by South Georgia Island, the South Sandwich Islands, the North Scotia Ridge, and the South Scotia Ridge. These topographic features show a close relationship with the distribution of seasonal maximum chlorophyll-*a* (Fig. 5b), clearly showing the topographic effects. Among the regions with topographic effects, particularly important is the wake of South Georgia in the South Georgia Basin, where the highest and prolonged blooms continue throughout austral summers.

The South Georgia Island region may have the most active natural iron fertilization in the SO. To the west of South Georgia, the Scotia Ridge deflects the ACC sharply northwards, where the SACCf loops anticyclonically around the island from the south, after which it resumes its easterly course (Nowlin and Klinck, 1986; Orsi et al., 1995).

We focus our analysis on a selected area in this region (dotted white rectangle in Fig. 5b). Fig. 10 shows monthly chlorophyll-*a* images from 1997/1998 to 2007/2008. The images show some interesting features. First, in most cases the blooms occur in the

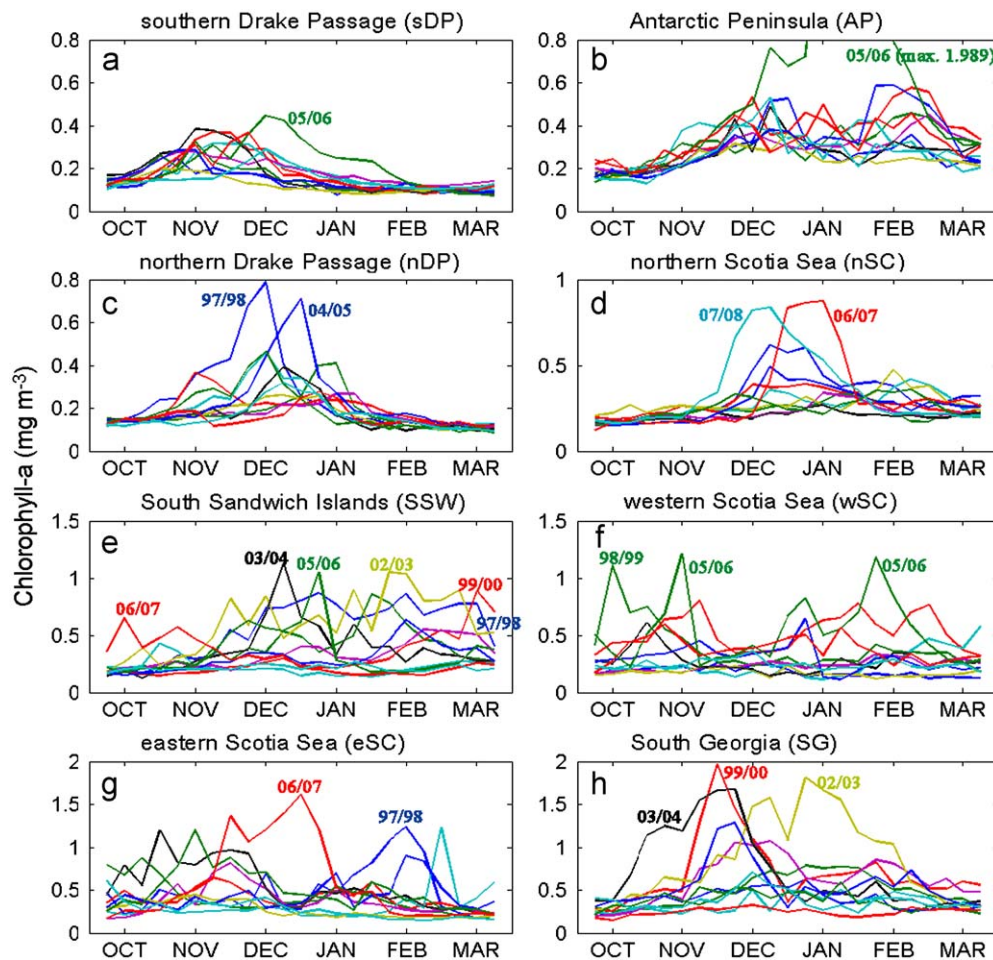


Fig. 6. Seasonal variations of the chlorophyll-*a* concentration in each region from 1997 to 2008. Here, 8-d composite chlorophyll-*a* data (median value of each region) were used. The 11-year chlorophyll-*a* concentrations are depicted by different colors (shades). Note that the vertical axes of chlorophyll-*a* have different scales.

wake of the South Georgia Island bounded by the PF and the SACCF. Second, the blooms can begin from October through December. Third, intense blooms can continue for 3–5 months. Fourth, the magnitude and timing of the blooms show large interannual variations (see also Fig. 8).

If the topographic effects result from the interaction of strong currents and topographic features, the topographic effects may be related to the current strength of the ACC. To test this hypothesis, we compared the monthly average of geostrophic current velocity with the monthly average chlorophyll-*a* concentration in the region. Fig. 11a shows the time series of monthly chlorophyll-*a* anomaly and geostrophic current velocity. Lower chlorophyll-*a* levels in 1997/1998, 1998/1999, 2000/2001, 2005/2006, and 2006/2007 match well with lower geostrophic current velocity. In addition, the higher chlorophyll-*a* levels in 1999/2000, 2002/2003, and 2003/2004 match well with lower geostrophic current velocity. The Pearson correlation coefficient between the two variables (for both variables, the normality assumption was accepted at the $p=0.05$ level) was significant ($p < 0.05$). To show the relationship more clearly, we calculated seasonal means of the chlorophyll-*a* and geostrophic current velocity and compared anomalies of these means (Figs. 11b, c). Higher chlorophyll-*a* years (1999/2000, 2001/2002, 2002/2003, and 2003/2004) match well with higher current velocity years, and vice versa. The Spearman correlation coefficient was 0.818, significant at a probability of 1% ($p=0.003$). We conclude that when the ACC in the SG region is stronger, the topographic effects are stronger.

4. Discussion

Analyses of ocean color data have revealed that seasonality is a prominent feature in the phytoplankton dynamics in the global ocean (Yoder et al., 1993; Banse and English, 1999; Obata et al., 1996; Longhurst, 2007; Yoo et al., 2008). The sea surface chlorophyll-*a* concentration generally responds to the seasonal cycles of solar energy, which affects the timing and intensity of vertical stability as well as vertical nutrient flux (Dandonneau et al., 2004). Longhurst (2007) showed that in all the four provinces in the SO (south of the sub-Antarctic Front), seasonality of surface chlorophyll-*a* was pronounced, with peaks in December–January. In our results, however, seasonality of the phytoplankton bloom was confined to the Drake Passage region. In other regions of the SASSO, weak (in the nSC) or no seasonality (in the AP, wSC, eSC, SG, and SSW) of phytoplankton blooms was evident. Thus, our findings are rather unexpected. We now seek a plausible explanation.

To understand the seasonal conditions of phytoplankton growth in the SASSO, we first examine the light condition. In austral summers, light intensity seems not to be a limiting factor, as the maximum integrated daily irradiance is about equal to that in the tropics during summer time (Campbell and Aarup, 1989). In Fig. 12, we calculated the critical depth in the eight regions using satellite-derived PAR and KPAR data and the formulation of Nelson and Smith (1991). The critical depths (broken lines) are shown for comparison with the MLD (solid lines). In the Drake

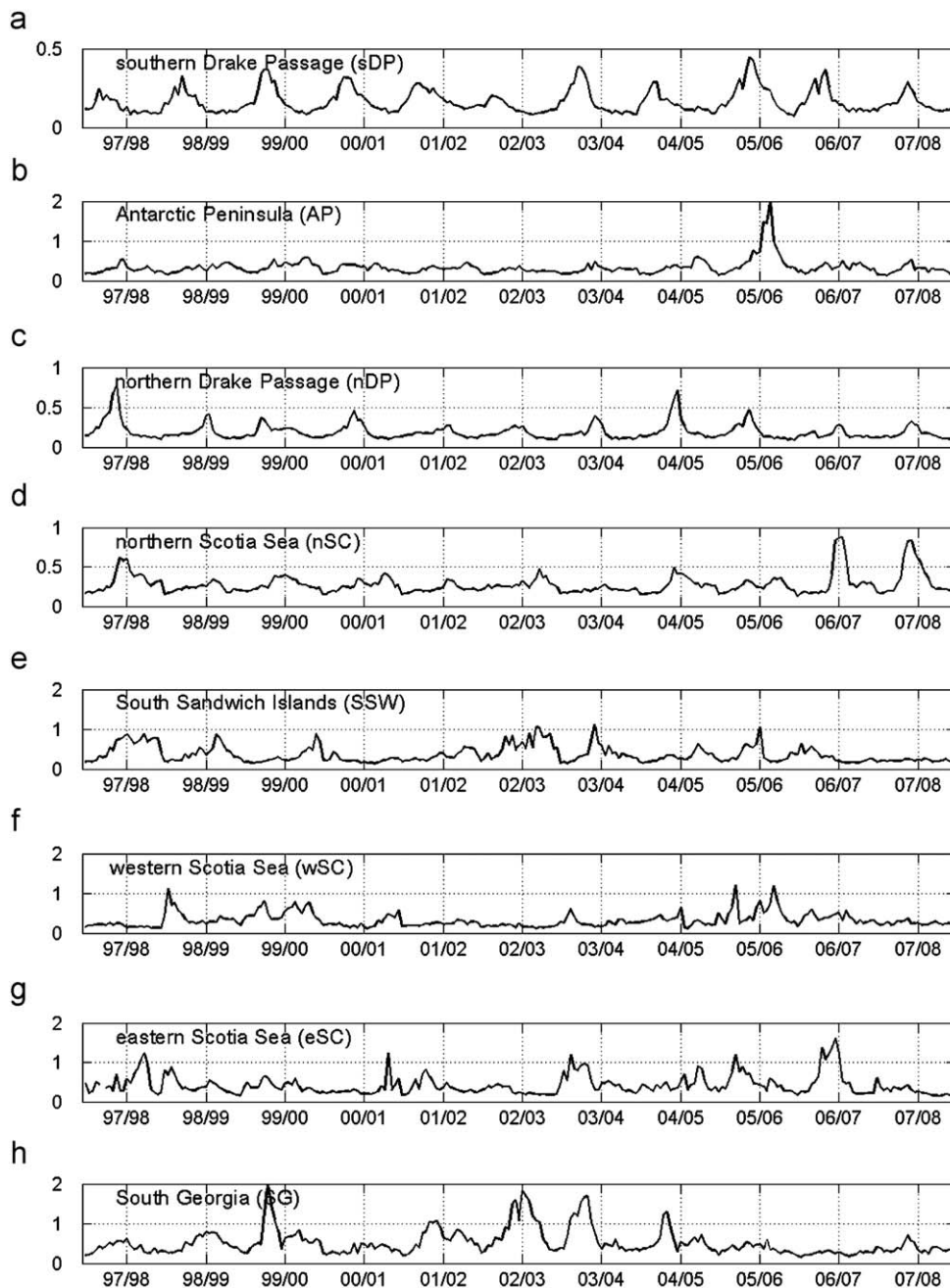


Fig. 7. Decadal-scale seasonal to interannual variations of chlorophyll-*a* in the eight regions from October 1997 to March 2008. Eight-day composite chlorophyll-*a* data were used. Note that only austral summertime data are shown (October to the following March). Grid lines indicate the first week of each year. Note that the vertical axes of chlorophyll-*a* have different scales.

Passage region, the critical depths became deeper than the MLD between October and November. This coincides well with the observed timing of regular spring blooms in the regions (November in the sDP and November–December in the nDP; Figs. 6–8). Therefore, light and nutrient conditions in the Drake Passage regions seem to be satisfied in the November–December period. In other regions, the critical depths became deeper than the MLD between September and October. Thus, the light condition in the UML would be satisfied for the net growth of phytoplankton populations in early spring. For example, in the Scotia Sea and South Georgia regions, the mean light condition in the UML exceeds the saturating light value for photosynthesis (I_k) in austral summer (Holm-Hansen et al., 2004). However, no significant relationship was found between the chlorophyll-*a*

concentration and the UML depth in these regions. Although the light condition is satisfied as early as September or October, in most cases, blooms appeared much later in the year (Fig. 6), suggesting that light is not the limiting factor but that nutrients might be.

Generally, macronutrients are not regarded as the limiting factor of the primary productivity in the SO because the SO has the largest inventory of unused macronutrients (Garcia et al., 2006). Following Martin et al. (1990), many researchers have suggested that low productivity in the nutrient-rich waters of the SO may result from a deficiency of iron. However, owing to difficulties of handling in situ iron samples, few results pertaining to the vertical distribution of dissolved iron have been published. Nonetheless, according to existing studies, the ferrocline in the

Table 1
Seasonal variability of chlorophyll-*a* and major hydrographic/geophysical characteristics of eight regions.

Regions	MLD (m)	Chlorophyll- <i>a</i>			Hydrographic/geophysical features	References
		Peak time (month)	Peak conc. (mg m ⁻³)	Seasonality		
sDP	25–294	Oct.–Dec.	0.199 (2002/2003)–0.446 (2005/2006)	Strong	<ul style="list-style-type: none"> Mild ACC current between PF and SACCF No topographical barrier and strong influence of the PF and SACCF Marginal Ice Zone 	
AP	22–177	Dec.–Feb.	0.361 (2002/2003)–0.588(2004/2005) 1.989 (2005/2006)*	None	<ul style="list-style-type: none"> Antarctic coastal current and Weddell Sea originated water^(a) Northern limit generally localized in the coastal region Sea ice is an important regulator of environments of surface water 	*Exceptional bloom Thorpe et al. (2007) ^(a)
nDP	42–327	Nov.–Jan.	0.262 (2002/2003)–0.786 (1997/1998)	Strong	<ul style="list-style-type: none"> Strong ACC current Narrow passing of ACC Deepest winter mixing Eddies are frequent 	
nSC	32–145	Dec.–Feb.	0.271 (2003/2004)–0.875 (2006/2007)	Weak	<ul style="list-style-type: none"> No intensive hydrographic study made Northern Scotia Ridge acts as a barrier to ACC flow 	
SSW	28–102	Oct.–Mar.	0.268 (2007/2008)–1.130 (2003/2004)	None	<ul style="list-style-type: none"> ACC does not affect this region Sea ice is more important In La Nina years, sea-ice retreat fast^(b) 	Stammerjohn et al. (2008) ^(b)
wSC	27–115	Oct.–Mar.	0.235 (2002/2003)–1.212 (2005/2006)	None	<ul style="list-style-type: none"> SFZ as a topographical barrier in the western boundary In the Ona Basin, anticyclonic meanders were observed^(c) Under the influence of the water from the shelf of the AP and the Weddell Sea^(d) Marginal Ice Zone 	Barre et al. (2008) ^(c) Whitworth et al. (1994) ^(d)
eSC	32–83	Oct.–Mar.	0.442 (2002/2003)–1.617 (2006/2007)	None	<ul style="list-style-type: none"> Weddell–Scotia Confluence Pirie Bank acts as a barrier to ACC flow Scotia Arc induces northward turn of ACC^(e) Marginal Ice Zone 	Thorpe et al. (2002) ^(e)
SG	30–91	Nov.–Jan.	0.327 (2006/2007)–1.972 (1999/2000)	None	<ul style="list-style-type: none"> Anticyclonic meandering of ACC due to South Georgia^(f) This anticyclonic flow around a bank of northwest South Georgia induces upwelling^(g) Island effects are strong because of SG Island and ridge 	Atkinson et al. (2001) ^(f) Brandon et al. (2000) ^(g)

The superscripts in 6th column indicate corresponding references in the 7th column.

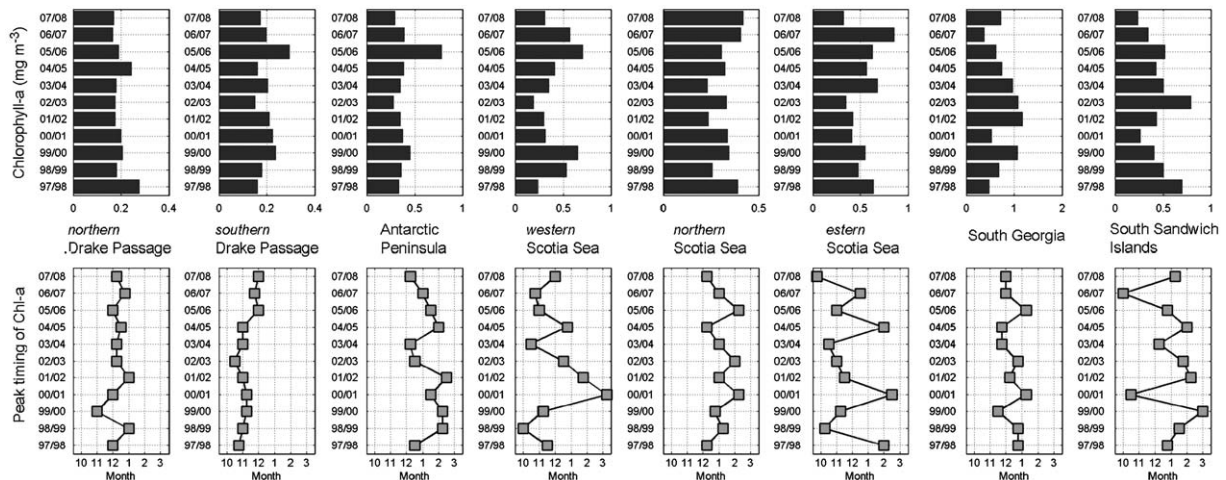


Fig. 8. Interannual variation of the seasonally averaged (October–March) chlorophyll-*a* concentration and peak timing of the seasonal maximum in chlorophyll-*a* from the 8-d time series. Note that the horizontal axes have different scales in the upper panels.

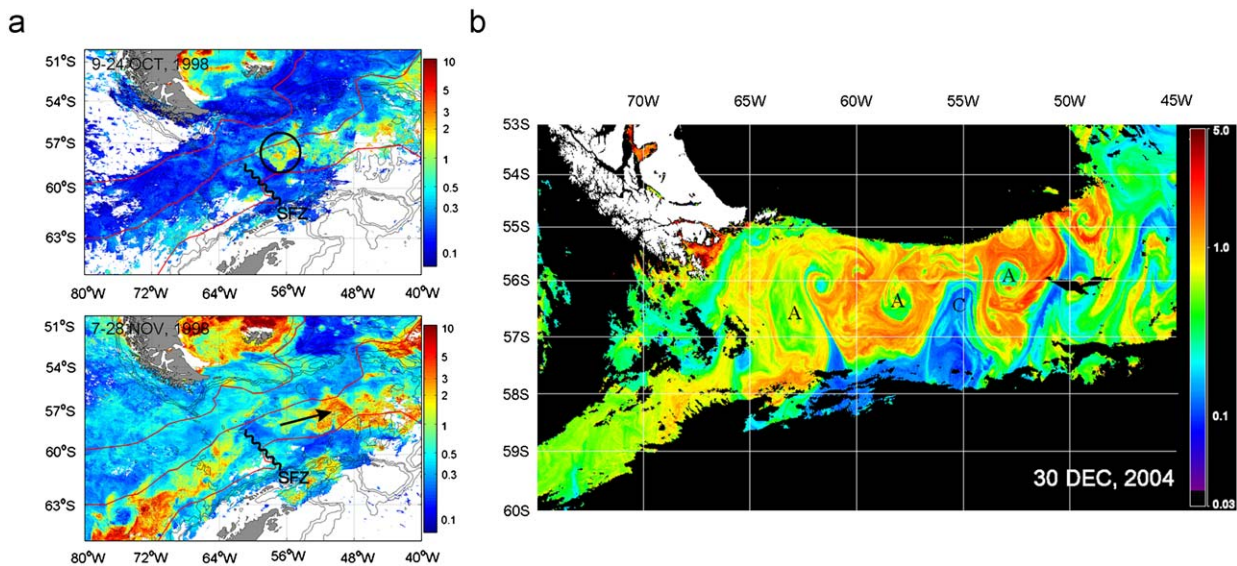


Fig. 9. (a) Composite images showing phytoplankton patches in the western Scotia Sea region from October to November 1998. The position of the Shackleton Fracture Zone is superimposed as a zigzag line. Major fronts are as in Fig. 5. (b) SeaWiFS images showing a string of cyclonic (C) and anticyclonic (A) eddies in the northern Drake Passage region on December 30, 2004.

study area forms around 200 m depth (Loscher et al., 1997), and the highest average iron concentrations in the UML were observed only in the PF and the SACCF regions (Measures and Vink, 2001).

Another aspect of Fig. 12 related to the nutrient supply is the difference in the maximum MLD. In the Drake Passage regions (the nDP and sDP), the maximum MLD was deeper than about 300 m, whereas in other regions, the MLD did not go deeper than 200 m. Therefore, in the Drake Passage region, deep winter mixing could entail entrainment of sub-surface waters enriched in iron (Measures and Vink, 2001), and hence, consistent blooms might occur when the light condition is favorable in spring (Nelson and Smith, 1991). On the other hand, the MLD did not deepen below the ferrocline in other regions (Fig. 12). For example, the climatology of the winter maximum of the MLD did not exceed 150 m in the Scotia Sea and South Georgia regions. Except for the Drake Passage, vertical mixing due to seasonal deepening of the UML does not seem to provide limiting nutrients to the UML. Thus, it is critical to reveal other mechanisms that bring nutrients to the UML. As shown in Section 3.5, topographic effects are the most important factor controlling the productivity in the SASSO region.

Topographic effects can increase upwelling of the upper Circumpolar Deep Water (CDW) along the SACCF, supplying micronutrients to the upper column and resulting in an increase of chlorophyll-*a* (de Baar et al., 1995; Loscher et al., 1997; Holm-Hansen et al., 2005; Meskhidze et al., 2007; Smith et al., 2008; see also Tynan, 1998; Holm-Hansen et al., 2004; and Marrari et al., 2008). Comiso et al. (1993) reported that the most significant relationship was a negative one between pigment levels and bathymetry. They interpreted this trend as indirect evidence for upwelling induced by topographical features that resulted in nutrient resupply to surface waters or the resuspension of iron (and algal cells) in shallow waters. Blain et al. (2007) recently studied such intensive natural iron fertilization on the Kerguelen Plateau. Their study revealed that the supply of iron and major nutrients from iron-rich deep water from below to the ocean surface was ten times higher than that in a short-term iron experiment.

Eddies are also part of the topographic effects (Fig. 9b). Naveira Garabato et al. (2004) described eddies and upwelling of deep

water in the Scotia Sea that are related to the complex bottom topography of this region. Letelier et al. (1997) hypothesized that the observed short-term variations of natural fluorescence in the PF region are a response of phytoplankton to the supply of limiting nutrients in the cyclonic eddy. Kahru et al. (2007) reported that the variability around South Georgia and the Scotia Sea may be induced by the cyclonic/anticyclonic eddy activity in the SACCF zone. They emphasized the role of cross-frontal mixing mediated by eddies in the increased productivity and chlorophyll-*a* concentration in the frontal zone.

We have shown that the topographic effects on chlorophyll-*a* were related to current speed. Therefore, to understand the causes of the interannual variation of chlorophyll-*a* in the South Georgia region, we should understand how the current intensity is controlled in that region.

One intriguing feature is that large-scale topographic effects were confined to the south of the PF in the ACC regions (see Section 3.5). This also coincides with krill distribution (Atkinson et al., 2004). The fact that the chlorophyll-*a* level to the north of the PF was low can be explained by the fact that nutrient-rich CDW upwells to the south of the PF and sinks in the north of the PF (Sarmiento et al., 2004). As a result, a pronounced meridional gradient in silicate concentration exists across the PF, high in the south and low in the north (Levitus et al., 1993; Garcia et al., 2006). We speculate that iron concentration may follow the same trend, and future in situ investigation could reveal whether this is the case.

Another factor of importance to phytoplankton dynamics in the SASSO is sea ice. The effect of sea ice on pelagic systems is threefold. First, light penetration into the water column is reduced, negatively affecting underlying pelagic production. Second, Martin et al. (1990) suggested that iron-rich airborne dust is deposited on the ice during winter, and as ice melts in spring, it releases this iron into the water, a process that accelerates the spring bloom (Smetacek and Nicol, 2005). Third, the growth and melting of sea ice affect the salinity of the upper ocean; hence water column stability and density gradients are changed. As sea ice has low salinity, ice melting in spring stabilizes the water column, which, in conjunction with increasing light, stimulates the development of dense phytoplankton blooms in the upper stratified water column (Sakshaug and

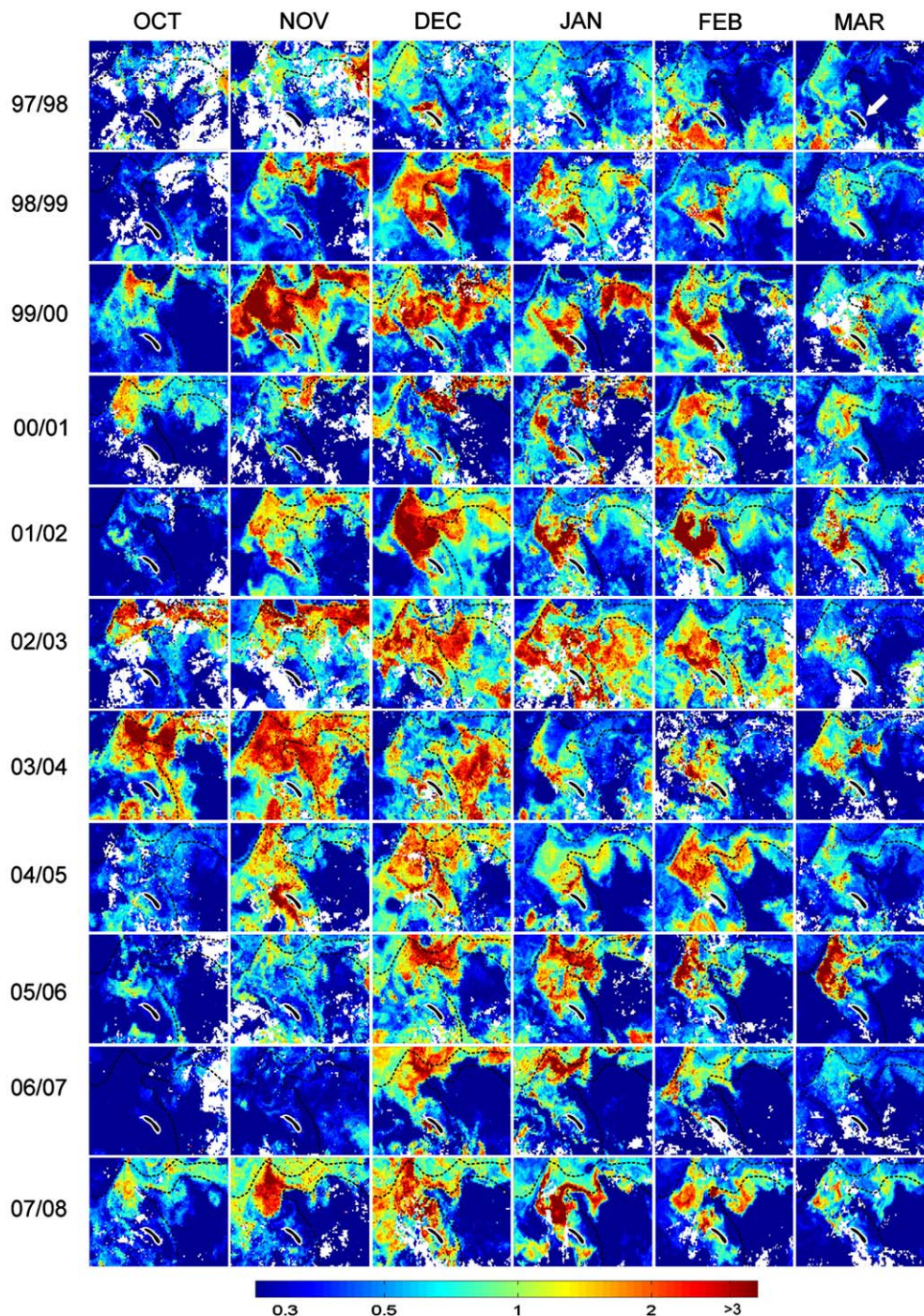


Fig. 10. Seasonal to interannual variations of the South Georgia phytoplankton blooms. The area is depicted by a white-dotted rectangle in Fig. 5b. The white arrow indicates South Georgia Island. The upper black dotted line denotes the approximate location of the PF, and the lower black dotted line denotes that of the SACC.

Holm-Hansen, 1984; Smith and Nelson, 1986). Consequently, sea-ice dynamics can mediate the timing and areal extent of phytoplankton production in the marginal ice zone (Smith et al., 2008; Vernet et al., 2008). It has been hypothesized that sea-ice melting is a trigger of phytoplankton bloom in polar regions (Kogeler and Rey, 1999; Qu et al., 2006). Many studies have reported that ice-edge blooms are related to spring ice-edge retreat in Antarctic waters (e.g., Sullivan et al., 1993; Siegel and Loeb, 1995; Arrigo and McClain, 1994; Smith et al., 1998; Garibotti et al., 2005; Williams et al., 2008; Vernet et al., 2008; see also Smith et al., 2008). However, Marrari et al. (2008) also

reported that, in the west AP region, chlorophyll values usually reached a maximum 4–6 weeks after the ice had receded. In Marguerite Bay, the summer bloom is dominated by large diatoms (Garibotti et al., 2003; Clarke et al., 2008), and the surface waters also exhibit the marked interannual variability, which is related to persistence/retreat of ice (Clarke et al., 2008; Marrari et al., 2008). Although this region shows high chlorophyll level, it was excluded in this study because valid chlorophyll-*a* data were limited for a detailed analysis (see Section 2).

The blooms in the sDP, AP, wSC, eSC, and SSW in 2005/2006 (Fig. 6) may exemplify blooms associated with ice retreat.

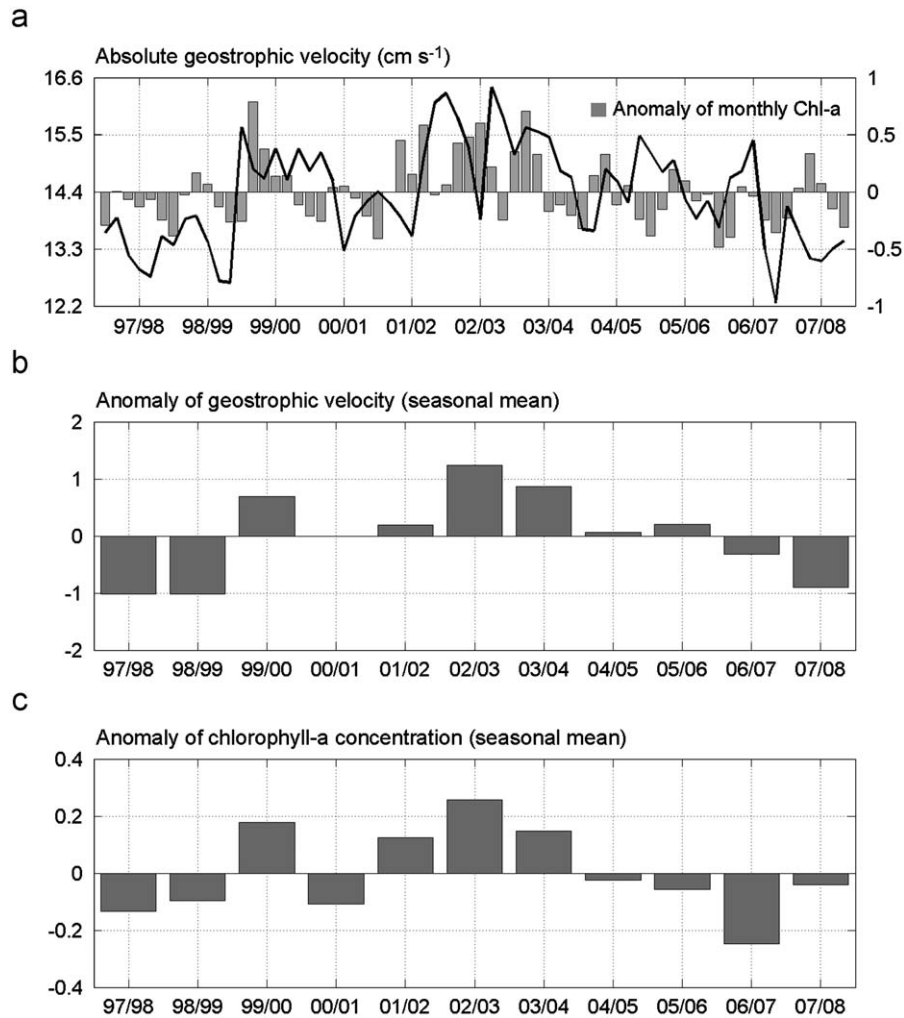


Fig. 11. Comparison of the geostrophic current and chlorophyll-*a* concentration anomaly for the South Georgia region delimited by the white-dotted line in Fig. 5b. (a) Geostrophic current velocity (line) and chlorophyll-*a* concentration anomaly (bars) on a monthly scale. The Pearson correlation coefficient between the two variables was significant ($P < 0.05$). (b) Anomaly of the seasonal means (October–March) of the geostrophic current velocity. (c) Anomaly of the seasonal means (October–March) of the chlorophyll-*a* concentration.

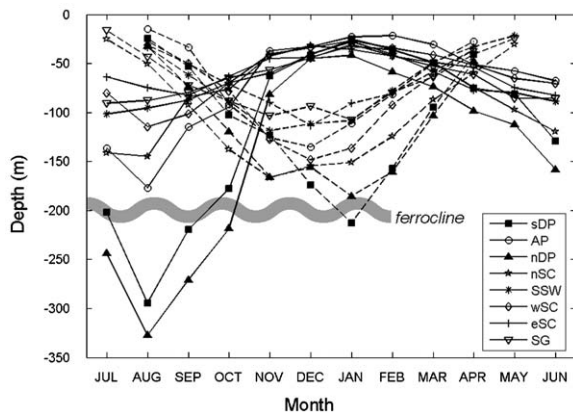


Fig. 12. Monthly change of mixed layer depth (solid lines) and critical depth (broken lines) in the eight regions. The critical depths were calculated from satellite PAR and KPAR data using the formulation of Nelson and Smith (1991).

In Fig. 13, blooms occurred after the ice edge receded at the AP and wSC in 2005/2006. This is in strong contrast with 2007/2008, when the ice had already receded to the coastline in October, and the chlorophyll-*a* concentration was low (Fig. 13, right panel).

The year 2005/2006 was a La Niña year. In La Niña years, strong and warm northerly winds promote sea-ice retreat in the western AP region in spring (Stammerjohn et al., 2008), leading to relatively high pigment (Smith et al., 2008).

To double-check other possible causes, we also examined irradiance, SST, and wind speed/direction in the AP region in 2005/2006. The integrated solar radiation was higher in 2007/2008 than that in 2005/2006, whereas SST did not differ much from other years. Time-averaged (December–February) SST during the 11 years ranged from 0.450 to 1.061 °C. The SST in 2005/2006 was somewhat high (1.020 °C), but the SST also was high in two other years (1.061 °C in 2001/2002 and 1.040 °C in 2006/2007). The southwesterly wind in the west of the AP may facilitate upwelling, which could have a considerable effect on the nutrient supply from below. From the 9-year QuikSCAT wind data, the year 2005/06 was peculiar in that southerly wind was very frequent, whereas it was negligible in other years (data not shown). This could potentially have enhanced upwelling to the west of the AP. However, on the basis of records collected between 1990 and 2007, the year 2005/2006 was one of 2 years when the UML depth was the shallowest and the average UML temperature was the warmest (Hewes et al., 2009). The relationship between stronger southerly wind and warming of the UML is not clear. It is also feasible that a favorable bloom condition is

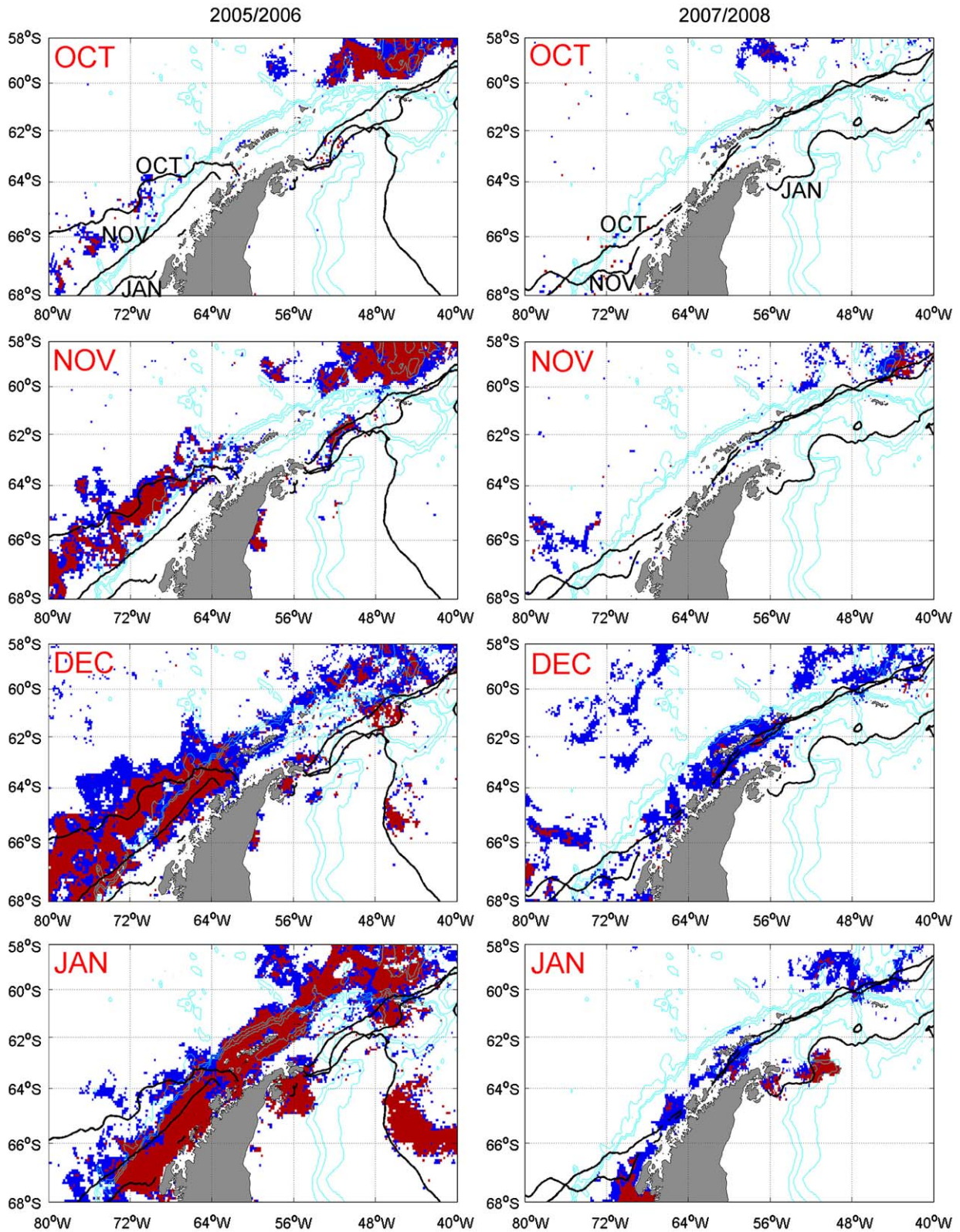


Fig. 13. Seasonal change of sea-ice extent and phytoplankton blooms in the AP and wSC regions in 2005/2006 and 2007/2008. The blue (dark grey) and red (grey) colors represent grid cells in which chlorophyll-*a* concentrations were higher than 0.5 and 1.0 mg m⁻³, respectively. Black lines indicate the mean sea-ice extent in October, November, and January.

buttressed by the stratification and shoaling of the UML with horizontal mixing of nutrient-rich water of Weddell Sea origin rather than vertical processes (Holm-Hansen et al., 1997; Hewes et al., 2008).

On a longer time scale, studies have shown strong co-variability between sea ice and climate indices such as ENSO indices throughout the South Pacific and the SASSO (Simmonds and Jacka, 1995; Yuan and Martinson, 2000; Venegas et al., 2001;

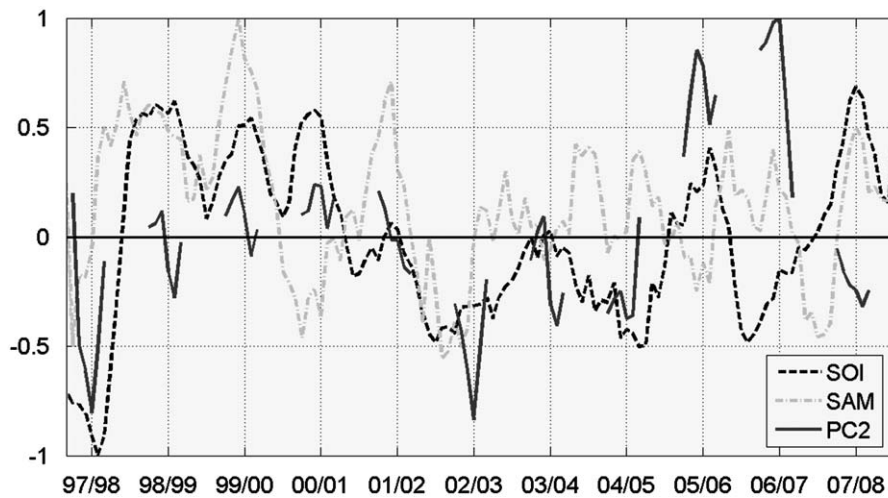


Fig. 14. The second EOF component (PC2 in Fig. 3) of monthly chlorophyll-*a* (solid line), the Southern Oscillation Index (SOI, dotted line), and the Southern Annular Mode (SAM, dash-dot line) versus time (September 1997 through August 2008). The SOI and SAM values are normalized by their minimum/maximum values for easier comparison with PC2. Note that all indices were smoothed by a 6-month running mean. The Spearman correlation coefficient between PC2 and SOI was significant ($P < 0.05$), whereas that between PC2 and SAM was not, for the period up to 2005/2006.

Kwok and Comiso, 2002; Arrigo and van Dijken, 2004). More recently, the high-latitude atmospheric ENSO response has appeared to have intensified (Smith et al., 2008; Meredith et al., 2008). Other modes of climate variability also occur in the SO. Among these, of particular interest is the SAM, which has been identified as the leading mode of atmospheric variability with a zonally symmetric dipole structure (Thompson and Wallace, 2000). The SAM plays an important role in determining SST variability at South Georgia (Marshall and Connolley, 2006; Meredith et al., 2008). The SAM also shows connections with negative and positive anomalies of sea-level pressure in the AP region (Stammerjohn et al., 2008), oceanic transport (Meredith et al., 2004; Yang et al., 2007), and CO₂ uptake (Lenton and Matear, 2007). Sen Gupta and England (2006) also argued that drag forces associated with the SAM anomalous surface wind and ocean circulation, as well as the various thermodynamic forcings, affect the advection and formation/melting of sea ice.

As the second component of EOFs (PC2 in Fig. 3) was interpreted to be related to blooms associated with ice retreat, we checked the relationship between PC2 and the SOI and SAM (Fig. 14). PC2 shows a trend similar to that of the SOI until 2005/2006. The Spearman correlation coefficient for the period up until 2005/06 was significant at a probability of 5% ($p=0.013$). However, the correlation coefficient between PC2 and the SAM for the same period was not significant. After 2005/2006, PC2 behaved differently from the SOI or SAM. PC2 was dominant in the sDP, wSC, and eSC regions, implying that ENSO signals primarily propagate east through the ACC (Meredith et al., 2005) and may affect sea-ice dynamics, particularly in the south of the PF. However, the change after 2005/2006 is not clear.

We have shown that chlorophyll-*a* variability in the SASSO is determined mainly by ACC and sea ice, which in turn are dependent on the climatological conditions of the region. Cavalieri et al. (1997) examined remote sensing data and reported that the areal extent of sea ice had decreased by $2.9 \pm 0.4\%$ decade⁻¹ in the Arctic Ocean during 1978–1996 but had increased by $1.3 \pm 0.2\%$ decade⁻¹ in the Southern Ocean during that time period. The increase in the Antarctic sea ice in spite of a warming trend in the Southern Hemisphere conforms with the recent increase in the length of the sea ice season in the SO from 1988 through 1994. In our study, both maximum speed and seasonal variation of wind in the SASSO decreased, especially in the higher latitudes, from 1997 to 2008 (data not shown).

This may not be the universal pattern in the SO, because Thompson and Solomon (2002) reported that the stronger southward-shifted westerly winds have prevailed over the SO, a pattern that has been associated with the intensification of the SAM in recent decades. According to Vaughan et al. (2001), the AP and Bellingshausen Sea region is among the three regions showing the largest temperature increases in the global ocean. A recent study by Montes-Hugo et al. (2009) also showed that summertime surface chlorophyll-*a* declined by 12% along the western Antarctic Peninsula over the past 30 years, especially at the northern part of the peninsula. Taken together, these findings suggest that it is very likely that meteorological and oceanographic conditions in the SO have been changing rapidly. If circulation and sea ice dynamics are among the major controlling factors of phytoplankton biomass in the SASSO, and if these factors are altered by climate change, it remains to be seen how the productivity in the SASSO ecosystems will change in the future.

Acknowledgements

The authors would like to thank the SeaWiFS Project and NASA for the production and distribution of SeaWiFS, MODIS, and QuikSCAT data, NSIDC for SSM/I data, AVISO for geostrophic current data, NOAA for AVHRR data, Bureau of Meteorology of Australian Government for SOI index, and NERC-BAS for SAM index. We are indebted to the comments and recommendations from two anonymous reviewers, which greatly helped to improve the paper. Suggestions from Prof. Young-Hyang Park on the earlier manuscript helped broaden the scope of the paper. This research was supported primarily by the KORDI Projects #PE98445 (POSEIDON) and #PM54970 (Research and applications of Geostationary Ocean Color Satellite). H.-C. Kim was also supported by KOPRI project #PG09030.

References

- Arrigo, K.R., McClain, C.R., 1994. Spring phytoplankton production in the Western Ross Sea. *Science* 266, 261–263.
- Arrigo, K.R., Worthen, D., Schnell, A., Lizotte, M.P., 1998. Primary production in Southern Ocean waters. *Journal of Geophysical Research* 103, 15587–15600.

- Arrigo, K.R., van Dijken, G.L., 2003. Phytoplankton dynamics within 37 Antarctic coastal polynya systems. *Journal of Geophysical Research*, doi:10.1029/2002JC001739.
- Arrigo, K.R., van Dijken, G.L., 2004. Annual changes in sea-ice, chlorophyll *a*, and primary production in the Ross Sea, Antarctica. *Deep-Sea Research II* 51, 117–138.
- Atkinson, A., Whitehouse, M.J., Priddle, J., Cripps, G.C., Ward, P., Brandon, M.A., 2001. South Georgia, Antarctica: a productive, cold water, pelagic ecosystem. *Marine Ecology Progress Series* 216, 279–308.
- Atkinson, A., Siegel, V., Pakhomov, E., Rothery, P., 2004. Long-term decline in krill stock and increase in salps within the Southern Ocean. *Nature* 432, 100–103.
- Atkinson, A., Siegel, V., Pakhomov, E.A., Rothery, P., Loeb, V., Ross, R.M., Quetin, L.B., Schmidt, K., Fretwell, P., Murphy, E.J., Tarling, G.A., Fleming, A.H., 2008. Oceanic circumpolar habitats of Antarctic krill. *Marine Ecology Progress Series* 362, 1–23.
- Banse, K., English, D.C., 1999. Seasonality of coastal zone color scanner phytoplankton pigment in the offshore oceans. *Journal of Geophysical Research* 99 (c4), 7323–7345.
- Barre, N., Provost, C., Sennechael, N., Lee, J.H., 2008. Circulation in the Ona Basin, southern Drake Passage. *Journal of Geophysical Research*, doi:10.1029/2007JC004549.
- Bathmann, U.V., Scharek, R., Klaas, C., Dubischar, C.D., Smetacek, V., 1997. Spring development of phytoplankton biomass and composition in major water masses of the Atlantic sector of the Southern Ocean. *Deep-Sea Research II* 44, 51–67.
- Blain, S., Queguiner, B., Armand, L., et al., 2007. Effect of natural iron fertilization on carbon sequestration in the Southern Ocean. *Nature* 446, 1070–1074.
- Bopp, L., Monfray, P., Aumont, O., Duffresne, J.L., Le Treut, H., Madec, G., Terray, L., Orr, J.C., 2001. Potential impact of climate change on marine export production. *Global Biogeochemical Cycles* 15, 81–99.
- Bracher, A.U., Kroon, B.M.A., Lucas, M.L., 1999. Primary production, physiological state and composition of phytoplankton in the Atlantic Sector of the Southern Ocean. *Marine Ecology Progress Series* 190, 1–16.
- Brandon, M.A., Murphy, E.J., Trathan, P.N., Bone, D.G., 2000. Physical oceanographic conditions to the northwest of the sub-Antarctic Island of South Georgia. *Journal of Geophysical Research* 105 (c10), 23983–23996.
- Brierley, A.S., Demer, D.A., Watkins, J.L., Hewitt, R.P., 1999. Concordance of interannual fluctuations in acoustically estimated densities of Antarctic krill around South Georgia and Elephant Island: biological evidence of same-year teleconnections across the Scotia Sea. *Marine Biology* 134, 675–681.
- Campbell, J.W., Aarup, T., 1989. Photosynthetically available radiation at high latitudes. *Limnology and Oceanography* 34, 1490–1499.
- Cavaliere, D.J., Gloersen, P., Parkinson, C.L., Comiso, J.C., Zwally, H.J., 1997. Observed hemispheric asymmetry in global sea ice changes. *Science* 278, 1104–1106.
- Chisholm, S.W., Morel, F.M.M., 1991. What controls phytoplankton production in nutrient-rich areas of the open sea? *Limnology and Oceanography* 36, 1507–1570.
- Clarke, A., Meredith, M.P., Wallace, M.I., Brandon, M.A., Thomas, D.N., 2008. Seasonal and interannual variability in temperature, chlorophyll and macronutrients in northern Marguerite Bay, Antarctica. *Deep-Sea Research II* 55, 1988–2006.
- Comiso, J.C., McClain, C.R., Sullivan, C.W., Ryan, J.P., Leonard, C.L., 1993. Coastal Zone Color Scanner pigment concentrations in the Southern Ocean and relationships to geophysical surface features. *Journal of Geophysical Research* 98 (c2), 2419–2451.
- Dandonneau, Y., Deschamps, P.Y., Nicolas, J.M., Loisel, H., Blanchot, J., Montel, Y., Thieuleux, F., Becu, G., 2004. Seasonal and interannual variability of ocean color and composition of phytoplankton communities in the North Atlantic, equatorial Pacific and South Pacific. *Deep-Sea Research II* 51, 303–318.
- De Baar, H.J.W., de Jong, J.T.M., Bakker, D.C.E., Loscher, B.M., Veth, C., Bathmann, U., Smetacek, V., 1995. Importance of iron for plankton blooms and carbon dioxide drawdown in the Southern Ocean. *Nature* 373, 412–415.
- De Boyer Montegut, C., Madec, G., Fischer, A.S., Lazar, A., Iudicone, D., 2004. Mixed layer depth over the global ocean: an examination of profile data and a profile-based climatology. *Journal of Geophysical Research*, doi:10.1029/2004JC002378.
- Dierssen, H.M., Vernet, M., Smith, R.C., 2000. Optimizing models for remotely estimating primary production in Antarctic coastal waters. *Antarctic Science* 12 (1), 20–32.
- DiTullio, G.R., Grebmeier, J.M., Arrigo, K.R., Lizotte, M.P., Robinson, D.H., Leventer, A., Barry, J.P., VanWoert, M.L., Dunbar, R.B., 2000. Rapid and early export of *Phaeocystis antarctica* blooms in the Ross Sea, Antarctica. *Nature* 404, 595–598.
- El-Sayed, S.Z., 2005. History and evolution of primary productivity studies of the Southern Ocean. *Polar Biology* 28, 423–438.
- Garcia, H.E., Locarnini, R.A., Boyer, T.P., Antonov, J.I., 2006. World Ocean Atlas 2005, vol. 4: Nutrients (phosphate, nitrate, and silicate). In: Levitus, S. (Ed.), NOAA Atlas NESDIS 64, US Government Printing Office, Washington, DC, 396pp.
- Garibotti, I.A., Vernet, M., Ferrario, M.E., Smith, R.C., Ross, R.M., Quetin, L.B., 2003. Phytoplankton spatial distribution patterns along the western Antarctic Peninsula (Southern Ocean). *Marine Ecology Progress Series* 261, 21–39.
- Garibotti, I.A., Vernet, M., Smith, R.C., Ferrario, M.E., 2005. Interannual variability in the distribution of the phytoplankton standing stock across the seasonal sea-ice zone west of the Antarctic Peninsula. *Journal of Plankton Research* 27 (8), 825–843.
- Gille, S.T., 2002. Warming of the Southern Ocean since the 1950s. *Science* 295, 1275–1277.
- Gloersen, P., Campbell, W.J., Cavalieri, D.J., Comiso, J.C., Parkinson, C.L., Zwally, H.J., 1992. Arctic and Antarctic Sea ice, 1978–1987: Satellite Passive Microwave Observations and Analysis. NASA Special Publication 511.
- Hewes, C.D., Reiss, C.S., Kahru, M., Mitchell, B.G., Holm-Hansen, O., 2008. Control of phytoplankton mixed layer depth in the western Weddell–Scotia Confluence. *Marine Ecology Progress Series* 366, 15–29.
- Hewes, C.D., Reiss, C.S., Holm-Hansen, O., 2009. A quantitative analysis of sources for summertime phytoplankton variability over 18 years in the South Shetland Islands (Antarctica) region. *Deep-Sea Research* 56, 1230–1241.
- Holm-Hansen, O., Hewes, C.D., Villafane, V.E., Helbling, E.W., Silva, N., Amos, T., 1997. Distribution of phytoplankton and nutrients in relation to different water masses in the area around Elephant Islands, Antarctica. *Polar Biology* 18, 145–153.
- Holm-Hansen, O., Naganobu, M., Kawaguchi, S., Kameda, T., Krasovskii, I., Tchernyshkov, P., Priddle, J., Korb, R., Brandon, M., Demer, D., Hewitt, R.P., Kahru, M., Hewes, C.D., 2004. Factors influencing the distribution, biomass, and productivity of phytoplankton in the Scotia Sea and adjoining waters. *Deep-Sea Research II* 51, 1333–1350.
- Holm-Hansen, O., Kahru, M., Hewes, C.D., 2005. Deep chlorophyll *a* maxima (DCMs) in pelagic Antarctic waters. II. Relation to bathymetric features and dissolved iron concentrations. *Marine Ecology Progress Series* 297, 71–81.
- Honjo, S., 2004. Particle export and the biological pump in the Southern Ocean. *Antarctic Science* 16 (4), 501–516.
- Kahru, M., Mitchell, B.G., Gille, S.T., Hewes, C.D., Holm-Hansen, O., 2007. Eddies enhance biological production in the Weddell–Scotia Confluence of the Southern Ocean. *Geophysical Research Letters* 34, L14603, doi:10.1029/2007GL030430.
- Kogeler, J., Rey, F., 1999. Ocean colour and the spatial and seasonal distribution of phytoplankton in the Barents Sea. *International Journal of Remote Sensing* 20 (7), 1303–1318.
- Korb, R.E., Whitehouse, M.J., Ward, P., 2004. SeaWiFS in the southern ocean: spatial and temporal variability in phytoplankton biomass around South Georgia. *Deep-Sea Research II* 51, 99–116.
- Kwok, R., Comiso, J.C., 2002. Southern Ocean climate and sea ice anomalies associated with the Southern Oscillation. *Journal of Climate* 15, 487–501.
- Lenton, A., Matear, R.J., 2007. Role of the Southern Annular Mode (SAM) in Southern Ocean CO₂ uptake. *Global Biogeochemical Cycles*, doi:10.1029/2006GB002714.
- Letelier, R.M., Abbott, M.R., Karl, D.M., 1997. Chlorophyll natural fluorescence response to upwelling events in the Southern Ocean. *Geophysical Research Letters* 24 (4), 409–412.
- Levitus, S., Konrigh, M.E., Reid, J.L., Najjar, R.G., Mantyla, A., 1993. Distribution of nitrate, phosphate and silicate in the world ocean. *Progress in Oceanography* 31, 245–273.
- Longhurst, A.R., 2007. Ecological geography of the sea, 2nd ed Academic Press.
- Loscher, B.M., de Baar, H.J.W., de Jong, J.T.M., Veth, C., Dehairs, F., 1997. The distribution of Fe in the Antarctic Circumpolar Current. *Deep-Sea Research II* 44 (1–2), 143–187.
- MacKay, D., 2003. Information Theory, Inference and Learning Algorithms. Cambridge University Press (pp. 284–292).
- Marrari, M., Hu, C., Daly, K., 2006. Validation of SeaWiFS chlorophyll *a* concentrations in the Southern Ocean: a revisit. *Remote Sensing of Environment* 105, 367–375.
- Marrari, M., Daly, K.L., Hu, C., 2008. Spatial and temporal variability of SeaWiFS chlorophyll *a* distributions west of the Antarctic Peninsula: implications for krill production. *Deep-Sea Research II* 55, 377–392.
- Marshall, G.J., 2003. Trends in the Southern Annular Mode from observations and reanalyses. *Journal of Climate* 16, 4134–4143.
- Marshall, G.J., Connolley, W.M., 2006. Effect of changing Southern Hemisphere winter sea surface temperatures on Southern Annular Mode strength. *Geophysical Research Letters*, doi:10.1029/2006GL026627.
- Martin, J.H., Gordon, R.M., Fitzwater, S.E., 1990. Iron in Antarctic waters. *Nature* 345, 156–158.
- McClain, C.R., Cleave, M.L., Feldman, G.C., Gregg, W.W., Hooker, S.B., Kuring, N., 1998. Science quality SeaWiFS data for global biosphere research. *Sea Technology* 39 (9), 10–16.
- Measures, C.I., Vink, S., 2001. Dissolved Fe in the upper waters of the Pacific sector of the Southern Ocean. *Deep-Sea Research II* 48, 3913–3941.
- Meredith, M.P., Watkins, J.L., Murphy, E.J., Ward, P., Bone, D.G., Thorpe, S.E., Grant, S.A., Larkin, R.S., 2003. Southern ACC Front to the northeast of South Georgia: pathways, characteristics, and fluxes. *Journal of Geophysical Research*, doi:10.1029/2001JC001227.
- Meredith, M.P., Woodworth, P.L., Hughes, C.W., Stepanov, V., 2004. Changes in the ocean transport through Drake Passage during the 1980s and 1990s, forced by changes in the Southern Annular Mode. *Geophysical Research Letters*, doi:10.1029/2004GL021169.
- Meredith, M.P., Brandon, M.A., Murphy, E.J., Trathan, P.N., Thorpe, S.E., Bone, D.G., Chernyshkov, P.P., Sushin, V.A., 2005. Variability in hydrographic conditions to the east and northwest of South Georgia, 1996–2001. *Journal of Marine Systems* 53 (1–4), 143–167.
- Meredith, M.P., Murphy, E.J., Hawker, E.J., King, J.C., Wallace, M.I., 2008. On the interannual variability of ocean temperatures around South Georgia, Southern

- Ocean: forcing by El Niño/Southern Oscillation and the Southern Annular Mode. *Deep-Sea Research II* 55, 2007–2022.
- Meskhidze, N., Nenes, A., Chameides, W.L., Luo, C., Mahowald, N., 2007. Atlantic Southern Ocean productivity: fertilization from above or below? *Global Biogeochemical Cycles*, doi:10.1029/2006GB002711.
- Meyer, B., Atkinson, A., Blume, B., Bathmann, U., 2003. Feeding and energy budgets of larval Antarctic krill *Euphausia superba* in summer. *Marine Ecology Progress Series* 257, 167–177.
- Mitchell, B.G., Holm-Hansen, O., 1991. Observations and modelling of the Antarctic phytoplankton crop in relation to mixing depth. *Deep-Sea Research* 38 (8–9), 981–1007.
- Montes-Hugo, M., Doney, S.C., Ducklow, H.W., Fraser, W., Martinson, D., Stammerjohn, S.E., Schofield, O., 2009. Recent changes in phytoplankton communities associated with rapid regional climate change along the western Antarctic Peninsula. *Science* 323, 1470–1473.
- Moore, J.K., Abbott, M.R., Richman, J.G., 1997. Variability in the location of the Antarctic Polar Front (90°–20°W) from satellite sea surface temperature data. *Journal of Geophysical Research* 102 (C13), 27825–27833.
- Moore, J.K., Abbott, M.R., 2000. Phytoplankton chlorophyll distributions and primary production in the Southern Ocean. *Journal of Geophysical Research* 105 (C12), 28709–28722.
- Murphy, E.J., Watkins, J.L., Trathan, P.N., Reid, K., Meredith, M.P., Thorpe, S.E., Johnston, N.M., Clarke, A., Tarling, G.A., Collins, M.A., Forcada, J., Shreeve, R.S., Atkinson, A., Korb, R., Whitehouse, M.J., Ward, P., Rodhouse, P.G., Enderlein, P., Hirst, A.G., Martin, A.R., Hill, S.L., Staniland, I.J., Pond, D.W., Briggs, D.R., Cunningham, N.J., Fleming, A.H., 2007. Spatial and temporal operation of the Scotia Sea ecosystem: a review of large-scale links in a krill centred food web. *Philosophical Transaction of the Royal Society B* 362, 113–148.
- Naveira Garabato, A.C.N., Polzin, K.L., King, B.A., Heywood, K.J., Visbeck, M., 2004. Widespread intense turbulent mixing in the Southern Ocean. *Science* 303, 210–213.
- Nelson, D.M., Smith Jr., W.O., 1991. Sverdrup revisited: critical depths, maximum chlorophyll levels, and the control of Southern Ocean productivity by the irradiance-mixing regime. *Limnology and Oceanography* 36 (8), 1650–1661.
- Nowlin Jr., W.D., Klinck, J.M., 1986. The physics of the Antarctic Circumpolar Current. *Reviews of Geophysics* 24, 469–491.
- Obata, A., Ishizaka, J., Endoh, M., 1996. Global verification of critical depth theory for phytoplankton bloom with climatological in situ temperature and satellite ocean color data. *Journal of Geophysical Research* 101, 20657–20667.
- Orsi, A.H., Whitworth III, T., Nowlin, W.D., 1995. On the meridional extent and fronts of the Antarctic Circumpolar Current. *Deep-Sea Research I* 42 (5), 641–673.
- Qu, B., Gabric, A.J., Matrai, P.A., 2006. The satellite-derived distribution of chlorophyll-*a* and its relation to ice cover, radiation and sea surface temperature in the Barents Sea. *Polar Biology* 29, 196–210.
- Sakshaug, E., Holm-Hansen, S., 1984. Factors governing pelagic production in polar oceans. In: Holm-Hansen, O. (Ed.), *Marine Phytoplankton and Productivity*. Springer, pp. 1–18.
- Sarmiento, J.L., Hughes, T.M.C., Stouffer, R.J., Manabe, S., 1998. Simulated response of the ocean carbon cycle to anthropogenic climate warming. *Nature* 393, 245–249.
- Sarmiento, J.L., Gruber, n., Brzezinski, M.A., Dunne, J.P., 2004. High-latitude controls of the thermocline nutrients and low latitude biological productivity. *Nature* 427, 56–60.
- Savidge, G., Harbour, D., Gilpin, L.C., Boyd, P.W., 1995. Phytoplankton distribution and production in the Bellingshausen Sea, Austral spring 1992. *Deep-Sea Research II* 42 (4–5), 1201–1224.
- Schlitzer, R., 2002. Carbon export fluxes in the Southern Ocean: results from inverse modeling and comparison with satellite-based estimates. *Deep-Sea Research II* 49, 1623–1644.
- Sen Gupta, A., England, M.H., 2006. Coupled ocean–atmosphere–ice response to variations in the Southern Annular Mode. *Journal of Climate* 19, 4457–4486.
- Siegel, V., Loeb, V., 1995. Recruitment of Antarctic krill *Euphausia superba* and possible causes for its variability. *Marine Ecology Progress Series* 123, 45–56.
- Siegel, V., 2005. Distribution and population dynamics of *Euphausia superba*: summary of recent findings. *Polar Biology* 29, 1–22.
- Simmonds, I., Jacka, T.H., 1995. Relationships between the interannual variability of Antarctic sea ice and the Southern Oscillation. *Journal of Climate* 8, 637–647.
- Smetacek, V., Nicol, S., 2005. Polar ocean ecosystems in a changing world. *Nature* 437 (15), 362–368.
- Smith Jr., W.O., Nelson, D.M., 1986. The importance of ice-edge phytoplankton production in the Southern Ocean. *BioScience* 36, 251–257.
- Smith, R.C., Baker, K.S., Vernet, M., 1998. Seasonal and interannual variability of phytoplankton biomass west of the Antarctic Peninsula. *Journal of Marine Systems* 17, 229–243.
- Smith, R.C., Martinson, D.G., Stammerjohn, S.E., Iannuzzi, R.A., Ireson, K., 2008. Bellingshausen and western Antarctic Peninsular region: pigment biomass and sea-ice spatial/temporal distributions and interannual variability. *Deep-Sea Research II* 55, 1949–1963.
- Stammerjohn, S.E., Martinson, D.G., Smith, R.C., Iannuzzi, R.A., 2008. Sea ice in the western Antarctic Peninsula region: spatio-temporal variability from ecological and climate change perspectives. *Deep-Sea Research II* 55, 2041–2058.
- Strass, V.H., Naveira Garabato, A.C., Pollard, R.T., Fischer, H.I., Hense, I., Allen, J.T., Read, J.F., Leach, H., Smetacek, V., 2002. Mesoscale frontal dynamics: shaping the environment of primary production in the Antarctic Circumpolar Current. *Deep-Sea Research II* 49, 3735–3769.
- Sullivan, C.W., Arrigo, K.R., McClain, C.R., Comiso, J.C., Firestone, J., 1993. Distributions of phytoplankton blooms in the Southern Ocean. *Science* 262, 1832–1837.
- Takahashi, T., Sutherland, S.C., Sweeney, C., Poisson, A., Metzl, N., Tilbrook, B., Bates, N., Wanninkhof, R., Feely, R.A., Sabine, C., Olafsson, J., Nojiri, Y., 2002. Global sea–air CO₂ flux based on climatological surface ocean pCO₂, and seasonal biological and temperature effects. *Deep-Sea Research II* 49, 1601–1622.
- Thompson, D.W.J., Wallace, J.M., 2000. Annular modes in the extratropical circulation. Part I: month-to-month variability. *Journal of Climate* 13, 1000–1016.
- Thompson, D.W.J., Solomon, S., 2002. Interpretation of recent southern hemisphere climate change. *Science* 296, 895–899.
- Thorpe, S.E., Heywood, K.J., Brandon, M.A., Stevnes, D.P., 2002. Variability of the southern Antarctic Circumpolar Current from north of South Georgia. *Journal of Marine Systems* 37, 87–105.
- Thorpe, S.E., Murphy, E.J., Watkins, J.L., 2007. Circumpolar connections between Antarctic krill (*Euphausia superba* Dana) populations: investigating the roles of ocean and sea ice transport. *Deep-Sea Research* 54, 792–810.
- Treguer, P., Nelson, D.M., van Benekom, A.J., DeMaster, D.J., Leynaert, A., Queguiner, B., 1995. The silica balance in the world ocean: a re-estimate. *Science* 268, 375–379.
- Tynan, C.T., 1998. Ecological importance of the Southern Boundary of the Antarctic Circumpolar Current. *Nature* 392, 708–710.
- Vaughan, D.G., Marshall, G.J., Connolley, W.M., King, J.C., Mulvaney, R., 2001. Devil in the detail. *Science* 293, 1777–1779.
- Venegas, S.A., Drinkwater, M.R., Schaffer, G., 2001. Coupled oscillations in Antarctic sea-ice and atmosphere in the South Pacific sector. *Geophysical Research Letters* 28 (17), 3301–3304.
- Vernet, M., Martinson, D., Iannuzzi, R., Stammerjohn, S., Kozłowski, W., Sines, K., Smith, R., Garibotti, I., 2008. Primary production within the sea-ice zone west of the Antarctic Peninsula: I—sea ice, summer mixed layer, and irradiance. *Deep-Sea Research II* 55, 2068–2085.
- Ward, P., Whitehouse, M., Meredith, M., Murphy, E., Shreeve, R., Korb, R., Watkins, J., Thorpe, S., Woodd-Walker, R., Brierley, A., Cunningham, N., Grant, S., Bone, D., 2002. The Southern Antarctic Circumpolar Current Front: physical and biological coupling at South Georgia. *Deep-Sea Research* 49, 2183–2202.
- Whitworth III, T., Nowlin Jr., W.D., Orsi, A.H., Locarmini, R.A., Smith, S.G., 1994. Weddell Sea Shelf in the Bransfield Strait and Weddell–Scotia Confluence. *Deep-Sea Research* 41, 629–641.
- Williams, G.D., Nicol, S., Raymond, B., Meiners, K., 2008. Summertime mixed layer development in the marginal sea ice zone off the Mawson coast, East Antarctica. *Deep-Sea Research II* 55, 365–376.
- Wulff, A., Wangberg, S.A., 2004. Spatial and vertical distribution of phytoplankton pigments in the eastern Atlantic sector of the Southern Ocean. *Deep-Sea Research II* 51, 2701–2713.
- Yang, X.Y., Wang, D., Wang, J., Huang, R.X., 2007. Connection between the decadal variability in the Southern Ocean circulation and the Southern Annular Mode. *Geophysical Research Letters*, doi:10.1029/2007GL030526.
- Yoder, J.A., McClain, C.R., Feldman, G.C., Esaias, W.E., 1993. Annual cycles of phytoplankton chlorophyll concentrations in the global ocean: a satellite view. *Global Biogeochemical Cycles* 7, 181–193.
- Yoo, S., Batchelder, H.P., Peterson, W.T., Sydeman, W.J., 2008. Seasonal, interannual and event scale variation in North Pacific ecosystems. *Progress in Oceanography* 77, 155–181.
- Yuan, X., Martinson, D.G., 2000. Antarctic sea ice extent variability and its global connectivity. *Journal of Climate* 13 (10), 1697–1717.